

MULTI BENEFIT RECHARGE PROJECT SIMPSON ROAD, CORNING

PREPARED FOR

TEHAMA COUNTY FCWCD
AND CORNING SUBBASIN GSA

PREPARED BY



TABLE OF CONTENTS

1. Introduction.....	4
2. Pilot Test #1.....	5
2.1. Site Information.....	5
2.2. Water Application.....	6
2.3. Methods	7
2.3.1. Water Balance	7
2.3.2. Depth Measurements	7
2.3.3. Precipitation and Evaporation.....	8
2.4. Data Analysis	8
2.4.1. Water Levels.....	8
2.4.2. Precipitation and Evaporation.....	10
2.5. Results	11
3. Pilot Test #2.....	11
3.1. Site Information.....	11
3.2. Water Application.....	12
3.3. Methods	13
3.3.1. Water Balance	13
3.3.2. Inflow Measurements	13
3.3.3. Precipitation and Evaporation.....	14
3.4. Data Analysis	14
3.4.1. Precipitation and Evaporation.....	14
3.5. Results	15
4. Geophysical Study.....	16
4.1. Methods	16
4.2. Data Analysis	17
4.3. Results	18
5. Conclusions and Recommendations	19

LIST OF TABLES

Table 2-3a OpenET Evaporation Rates.....	10
Table 2-3b Drawdown Event Evaporation Rates	10
Table 2-4 Infiltration Rates	11

TABLE OF CONTENTS

Table 3-3a Precipitation Volume	15
Table 3-3b Evapotranspiration (ET) Volume	15
Table 3-4a Infiltration Volume and Rate.....	15

LIST OF FIGURES

Figure 1-1. Recharge Pilot Test Areas	5
Figure 2-1. Pilot Test #1 Basin Aerial View Looking Southeast.....	6
Figure 2-2. CWD Irrigation Infrastructure and Water Flowing into the Basin	7
Figure 2-3a. Water Level During First Drawdown Event- May 29, 2024 to May 30, 2024	9
Figure 2-3b. Water Level During Second Drawdown Event- June 6, 2024 to June 7, 2024.....	9
Figure 3-1. Pilot Test #2 Basin Aerial View Looking Northwest.....	12
Figure 3-2. Pilot Test #2 Basin Showing Pipeline and Outlets.....	13
Figure 3-3. Corning Water District Meter	14
Figure 4-1. tTEM Survey Lines.....	17
Figure 4-2. Scale Used to Represent Resistivity Values in Report	18
Figure 4-3 Mean Resistivity Plan-view Map Series	19

APPENDICES

Appendix A	tTEM Geophysical surveys Esteve Property, Corning, California
Appendix B	Vegetation and Wildlife Photos

TABLE OF CONTENTS

LIST OF ACRONYMS AND ABBREVIATIONS

Acronym	Meaning
AF	Acre-foot
CIMIS	California Irrigation Management Information System
CWD	Corning Water District
ET	Evapotranspiration
GSA	Groundwater Sustainability Agency
TNC	The Nature Conservancy
tTEM	Towed Transient Electromagnetic

1. INTRODUCTION

This feasibility study was conducted as part of the Tehama County GSP Implementation Prop 68 Grant under the Multi Benefit Recharge task. The study site is located in the Corning Subbasin and consists of two fallow fields, one approximately 30 acres and the other approximately 73 acres on the south side of Thomes Creek (**Figure 1-1**). This study area was considered an ideal location for potential recharge and habitat enhancement as it satisfied the following criteria:

- 1) Currently fallow,
- 2) Access to water from Corning Water District (CWD),
- 3) Located in an area with little surface water during the late summer and early fall.

From May through November 2024, two pilot tests were conducted on the property to determine the feasibility of conducting multi-benefit recharge at the site. An initial, small-scale, pilot test was conducted from late May to early June to determine the viability of the site for infiltration. Following the positive results of the initial test, The Nature Conservancy (TNC) assisted in a second pilot test to further evaluate the site's potential to provide habitat for shorebird populations. The test occurred during the late summer and fall time period when shallow water habitat for shorebirds is limited. This scaled-up pilot test applied a larger volume of water over a larger area from September through November.

In January 2025, a geophysical study was conducted in and around the area of Pilot Test #2. The study consisted of a towed Transient Electromagnetic (tTEM) survey of the site conducted by Geophysical Imaging Partners. Results of the study were used to evaluate the fate of infiltrated water and identify subsurface flow paths beneath the site.

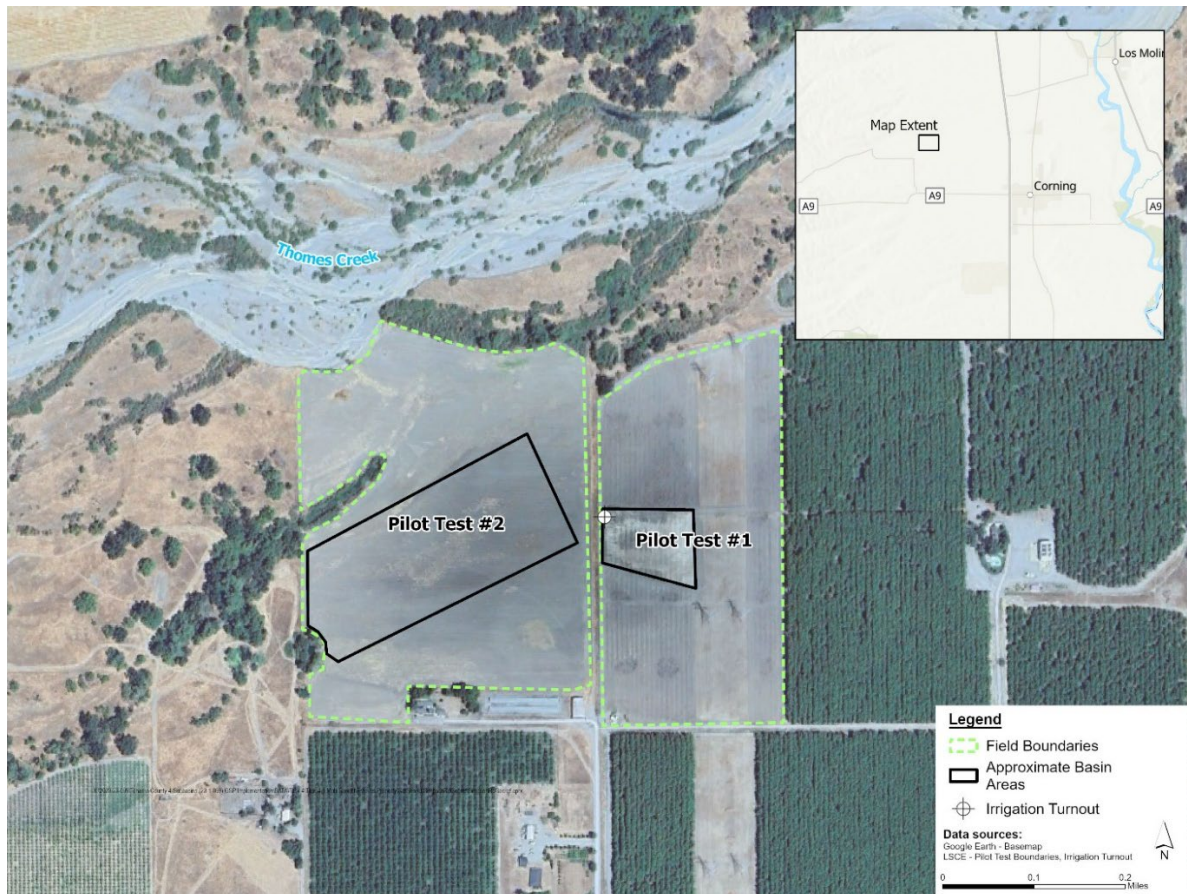


Figure 1-1. Recharge Pilot Test Areas

2. PILOT TEST #1

2.1. Site Information

The first pilot test took place on the 30-acre field on the eastern portion of the site. This field was historically planted with walnuts, but half the trees under high-voltage power lines were removed between 2013 and 2015 under an agreement with the power company. Later, between 2022 and 2024, the walnuts on the remaining portion of the field were removed as well. Since that time, the field has remained fallow, with periodic disking to control weeds. During the pilot test, the field had recently been disced and was generally free of vegetation. The field was not perfectly level during the pilot test, however the variation in elevation across the site varied only slightly. To keep water contained during the pilot test, a small basin of approximately 2.9 acres was created by a short berm (about 2 feet tall) immediately adjacent to the Corning Water District irrigation turnout (**Figure 2-1**).



Figure 2-1. Pilot Test #1 Basin Aerial View Looking Southeast

2.2. Water Application

For this pilot test, surface water obtained from CWD was directed into the basin from the existing turnout in the northwest corner of the basin. Water from the turnout was allowed to flow freely into the basin and spread (**Figure 2-2**). Due to the slight change in elevation across the site, the water tended to flow towards the eastern end of the basin. A total of 15 AF of water was applied during pilot test #1.



Figure 2-2. CWD Irrigation Infrastructure and Water Flowing into the Basin

2.3. Methods

2.3.1. Water Balance

A water balance method was employed to determine the percolation rate of the location. This method involves accounting for inflows and outflows and calculating the resulting change in water level in the pond. Inflows include applied water from the Corning Water District infrastructure, plus any precipitation. Outflows consist of infiltration of the water into the subsurface as well as evaporation. During this pilot test, inflows were accounted for by depth measurements, and precipitation was measured by a nearby California Irrigation Management Information System (CIMIS) station. Outflows were accounted for by the same depth measurements and evaporation was measured using data from OpenET. The total drawdown rate measured at the transducer, plus the rate of precipitation, minus the rate of evaporation, to yield the actual infiltration rate.

2.3.2. Depth Measurements

A water depth transducer within a slotted length of PVC pipe was installed at a location at the basin's anticipated deepest point.

On May 28, 2024, the valve on the irrigation turnout was opened, initiating the basin's first period of rapid filling. By the following day, May 29, 2024, the basin was partially drained to observe drawdown and evaluate its infiltration capacity from a dry state.

Subsequently, on May 30, 2024, the basin was refilled and maintained at near-full capacity until June 6, 2024, when it was fully drained. Complete drainage occurred by noon on June 7, 2024. During this period, drawdown was recorded again to assess infiltration under saturated conditions.

2.3.3. Precipitation and Evaporation

Precipitation during the pilot test was expected to be minimal to non-existent. A nearby CIMIS station, Gerber South #222, approximately 8.3 miles away, measured no precipitation during the initial filling and drawdown of the basin. During the second filling and drawdown period, a total of 0.01 inches of precipitation was recorded on June 3, 2024. As this precipitation did not occur during either of the two drawdown phases, it was not considered as an inflow in the results.

Evaporation data for the pilot test period was obtained from OpenET field summary data, which uses satellite imagery to calculate daily evapotranspiration (ET) rates. The basin area was selected via the website's user interface to determine the daily ET rate. This rate was then converted to an average hourly rate for comparison with water depth data. Since the basin was largely free of vegetation during the test, the ET rate is assumed to represent evaporation only, with no contribution from plant transpiration.

2.4. Data Analysis

2.4.1. Water Levels

Data collected from the transducer deployed at the deepest part of the basin was analyzed during the first and second drawdown events. Depth data were collected at 15-minute intervals and plotted (**Figure 2-3a and Figure 2-3b**). A best fit line was generated to determine the approximate water infiltration rate in both inches per hour and feet per day for both drawdown events. During the first drawdown under dry conditions, the drawdown rate was calculated at 0.93 in/hr or 1.86 ft/day. For the second drawdown under saturated conditions, the drawdown rate was calculated at 0.77 in/hr or 1.54 ft/day.

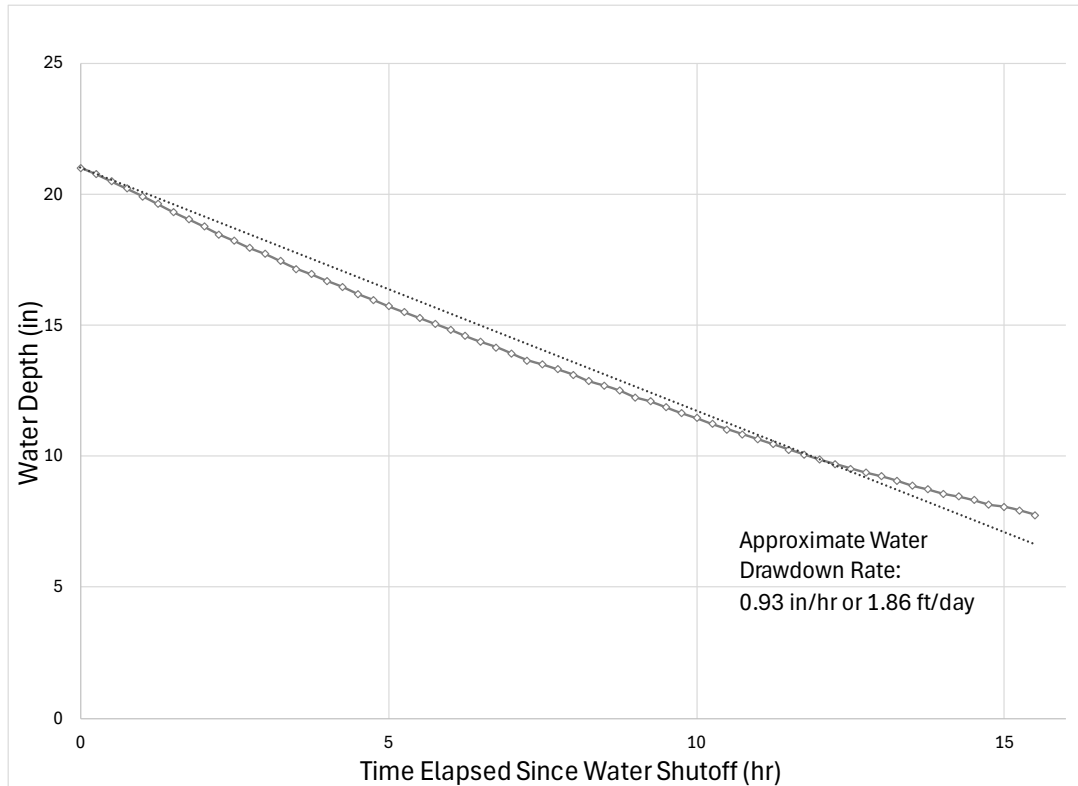


Figure 2-3a. Water Level During First Drawdown Event- May 29, 2024 to May 30, 2024

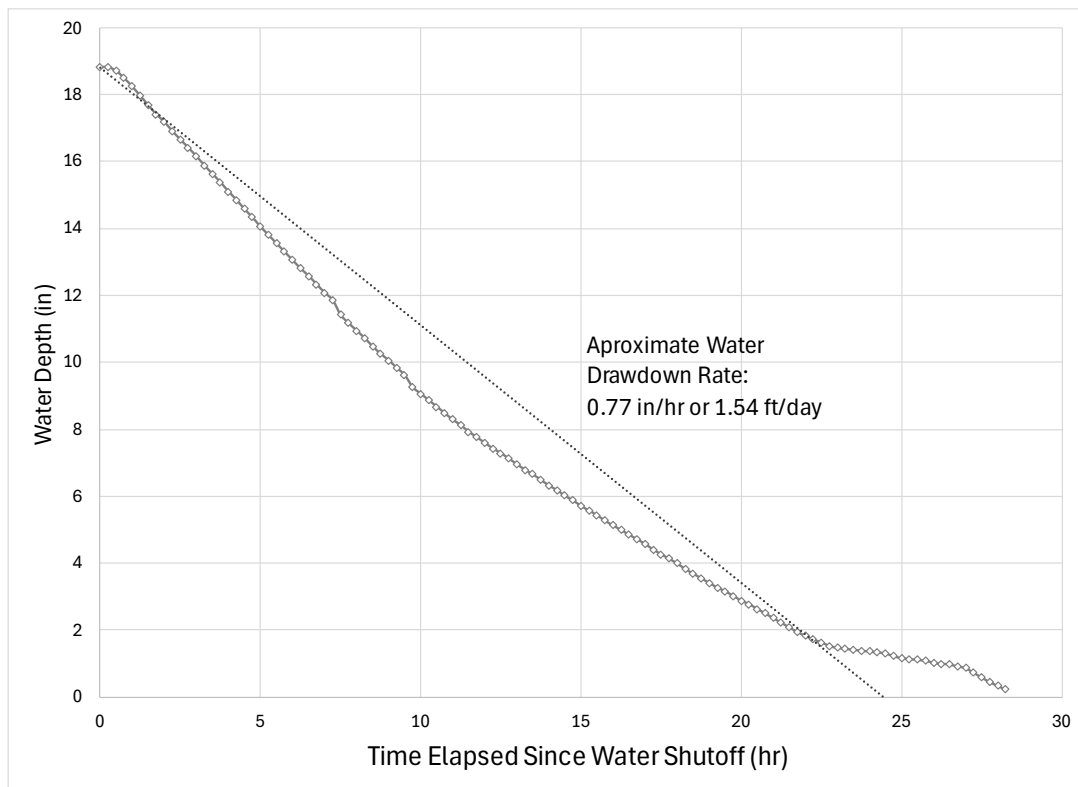


Figure 2-3b. Water Level During Second Drawdown Event- June 6, 2024 to June 7, 2024

2.4.2. Precipitation and Evaporation

As stated previously, precipitation during this pilot test was so slight that it was not considered as an inflow.

Evaporation data were obtained through the user interface on OpenET for the duration of the pilot test. Hourly evaporation rates for each day were calculated based on the daily rates obtained. **Table 2-3a** shows the daily and average hourly evaporation rate for each day of the pilot test. It is important to note that evaporation rates vary throughout the day, with higher rates experienced during the daytime hours and lower rates at night. However, this variation has a limited impact on final results. As both drawdown events occurred over the course of two days, the average ET over the course of each of those drawdown events were calculated, shown in **Table 2-3b**. The average daily and hourly evaporation rates for each drawdown event were subtracted from the infiltration rates derived from the best-fit lines to isolate the portion of the drawdown attributable to subsurface infiltration.

Table 2-3a OpenET Evaporation Rates		
Date	ET Rate (in/hr)	ET Rate (ft/day)
5/28/2024	0.002676	0.00535105
5/29/2024	0.004313	0.008625328
5/30/2024	0.005792	0.011584646
5/31/2024	0.005335	0.010669291
6/1/2024	0.003133	0.006266404
6/2/2024	0.002754	0.00550853
6/3/2024	0.002744	0.005488845
6/4/2024	0.006117	0.012234252
6/5/2024	0.006362	0.012723097
6/6/2024	0.005105	0.010209974
6/7/2024	0.005402	0.010803806

Table 2-3b Drawdown Event Evaporation Rates		
Drawdown Event	Average ET Rate (in/hr)	Average ET Rate (ft/day)
Event 1: 5/29/2024 – 5/30/2024	0.005052	0.010105
Event 2: 6/6/2024 – 6/7/2024	0.005253	0.010507

2.5. Results

As described in Section 2.3.1, the actual infiltration rate of water into the subsurface is determined by the measured drawdown rate at the transducer, plus the precipitation rate (in this case zero), minus the evaporation rate, yielding the final infiltration rate. The final infiltration rate for the first event, under dry conditions, was 0.92 in/hr or 1.85 ft/day. The infiltration rate for the second event, under saturated conditions, was 0.77 in/hr or 1.53 ft/day. The calculations for each of the two drawdown events are summarized in **Table 2-4** below. Overall, the rate of evaporation is minimal when compared to the overall drawdown rate, resulting in total infiltration being only slightly lower than the total drawdown rate, suggesting a high recharge potential at this location.

Table 2-4 Infiltration Rates					
Drawdown Event	Drawdown Rate (in/hr)	Precipitation Rate (in/hr)	Evaporation Rate (in/hr)	Infiltration Rate (in/hr)	Infiltration Rate (ft/day)
Event 1: 5/29/2024 – 5/30/2024	0.928	0.00	0.005052	0.92	1.85
Event 2: 6/6/2024 – 6/7/2024	0.7704	0.00	0.005253	0.77	1.53

3. PILOT TEST #2

3.1. Site Information

The field for the second pilot test was approximately 42 acres and was located immediately to the west of the field used in pilot test #1. Based on a review of historical satellite imagery of the area, prior to 2015, this was utilized for grazing, with some cross fencing and scattered trees on the property. Since 2015, the field has remained fallow or has been planted in short-duration annual crops. At the start of the pilot test, the field had recently been disced and was largely free of vegetation. Like the field in pilot test #1, this site was uneven, sloping gently to the north toward Thomes Creek. This test site also had a basin created by a short berm, similar to pilot test #1. Furthermore, additional berms were created within the basin to address the change in elevation and help distribute water across the site. (**Figure 3-1**).

Prior to the start of the pilot test, TNC evaluated the site to determine if it was appropriate to provide habitat shorebird species. The site was located an appropriate distance from power lines and trees which could provide a perch for predator bird species such as hawks and falcons. Additionally, the timing of the pilot test in the late summer and early fall timeframe was selected to provide habitat during a season when shallow water is not widespread in the area.



Figure 3-1. Pilot Test #2 Basin Aerial View Looking Northwest

3.2. Water Application

Water delivery followed a similar method as in the first test, using the same CWD irrigation turnout. A temporary pipeline with multiple outlet points directed water from the irrigation turnout to the site and distributed it across the basin (**Figure 3-2**). During this pilot test, 271 acre-feet of surface water procured from CWD was applied to the site. The cost of the water applied during the pilot test was \$21,737.60. The funding to purchase the water from CWD was provided by TNC.



Figure 3-2. Pilot Test #2 Basin Showing Pipeline and Outlets

3.3. Methods

3.3.1. Water Balance

A similar water balance method to the first pilot test was employed to determine the infiltration rate during this subsequent test. As before, this method involved accounting for inflows and outflows to the basin. Inflows include applied water from the Corning Water District infrastructure, plus any precipitation. Outflows consisted of subsurface water infiltration and evaporation. During this pilot test, inflows were accounted for by meter readings from the Corning water District infrastructure, and precipitation was measured by the same California Irrigation Management Information System (CIMIS) station as the previous test. Outflows were accounted for by determining evaporation using data from OpenET, with the remainder attributed to subsurface infiltration.

3.3.2. Inflow Measurements

During this test, the water within the basin was to be kept shallow to provide ideal habitat for selected bird species. Due to the shallow water, measuring water level with transducers was not practical. Meter readings were taken at the beginning and end of the test to determine the total volume of water applied, measured in acre-feet (see **Figure 3-3**). Water was applied continuously to the site from September 13, 2024 through November 13, 2024. However, there were a few instances of the water flow rate into the basin being increased, decreased, or fully stopped to allow for maintenance of the berm surrounding the basin.



Figure 3-3. Corning Water District Meter

3.3.3. Precipitation and Evaporation

Precipitation during this second pilot test was again expected to be slight. The same nearby CIMIS station, Gerber South #222, was used to determine precipitation amounts. Precipitation rates from CIMIS were provided in inches per day. To determine the total volume (in acre-feet) of precipitation into the basin, this rate was multiplied by the total size of the wetted area of the basin. The size of the wetted area was calculated by utilizing Sentinel-2 satellite imagery.

Evaporation data for the time period of the pilot test was obtained through the OpenET field user interface. In this test, the daily ET values were totaled over the duration of the pilot test to determine the total evaporation from the basin. Similarly to precipitation, the total volume of water evaporated from the basin was calculated by multiplying the ET rate (in inches per day) by the wetted area (in acres). In this test, it was assumed that the ET rate includes both evaporation and transpiration from vegetation that began growing around the perimeter soon after the water was applied to the basin.

3.4. Data Analysis

3.4.1. Precipitation and Evaporation

The nearby CIMIS station, Gerber South #222, was used to determine precipitation amounts into the basin. Precipitation rates from CIMIS were multiplied by the total size of the wetted area in the basin, which was calculated by utilizing Sentinel-2 satellite imagery. The size of the wetted area varied over the course of the pilot test, so the average of the wetted area from September 20, 2024, October 13, 2024 and November 7, 2024 was used for the calculations. The calculated volume for precipitation into the basin over the period of the test was 0.69 acre-feet and is summarized in **Table 3-3a** below.

Table 3-3a Precipitation Volume			
Time Period	Total Precipitation (ft)	Wetted Area (acres)	Total Precipitation Volume (ac-ft)
9/13/2024 – 11/13/2024	0.1575	4.36	0.69

ET data were obtained through the user interface on OpenET for the duration of the pilot test. The total ET (in feet) was calculated by summing ET from September 13, 2024, through November 13, 2024. This value was multiplied by the average wetted area to determine the total volume of water lost to ET, which was 0.92 acre-feet and is summarized in **Table 3-3b** below.

Table 3-3b Evapotranspiration (ET) Volume			
Time Period	Total ET (ft)	Wetted Area (acres)	Total ET Volume (ac-ft)
9/13/2024 – 11/13/2024	0.211	4.36	0.92

3.5. Results

As stated previously, determining the total infiltration and the infiltration rate for the second pilot test involved accounting for inflows and outflows to the basin. Inflows included applied water from the Corning Water District infrastructure, plus any precipitation. Outflows consisted of infiltration of the water into the subsurface as well as evaporation. Therefore, the total volume of water infiltrated into the subsurface was calculated by adding the total volume of water applied as measured at the meter and the volume of water from precipitation and subtracting the volume of water lost to ET. These values are summarized in **Table 3.4a**. The total amount infiltrated over the course of the pilot test was 270.77 acre-feet. As the pilot test ran for a total of 62 days, this volume yielded a rate of 4.37 ac-ft/day (or 1.0 ft/day over 4.36 acres). The 62-day time frame utilized for the infiltration rate calculation included several days with no flow into the basin. Thus, the actual infiltration rate is expected to be slightly higher than the calculated rate.

Table 3-4a Infiltration Volume and Rate				
Applied Water Volume (ac-ft)	Precipitation Volume (ac-ft)	ET Volume (ac-ft)	Infiltration Volume (ac-ft)	Infiltration Rate (ac-ft/day)
271.0	0.69	0.92	270.77	4.37

4. GEOPHYSICAL STUDY

4.1. Methods

Following the successful completion of Pilot Tests 1 and 2, a geophysical study of the area was conducted. The study consisted of a towed Transient Electromagnetic (tTEM) survey of the site conducted by Geophysical Imaging Partners. The tTEM system utilizes a sled towed behind an all-terrain vehicle which induces an electromagnetic field into the ground and subsequently measures the electrical resistivity of the subsurface materials. The sled was pulled across the property in east-west trending parallel lines spaced approximately 30m (~100ft) apart to characterize the subsurface across the entire property. Additional readings were also taken in dry portions of Thomes Creek for comparison as shown in **Figure 4-1**. The resistivity of the subsurface materials gives an indication of the granularity of the materials. Areas of high resistivity generally having more coarse-grained materials (sands and gravels), and areas with low resistivity having fine-grained materials (silts and clays). A detailed description of the methods used in the survey can be found in the Introduction and Field Operations sections of **Appendix A: tTEM Geophysical surveys Esteve Property, Corning, California**.

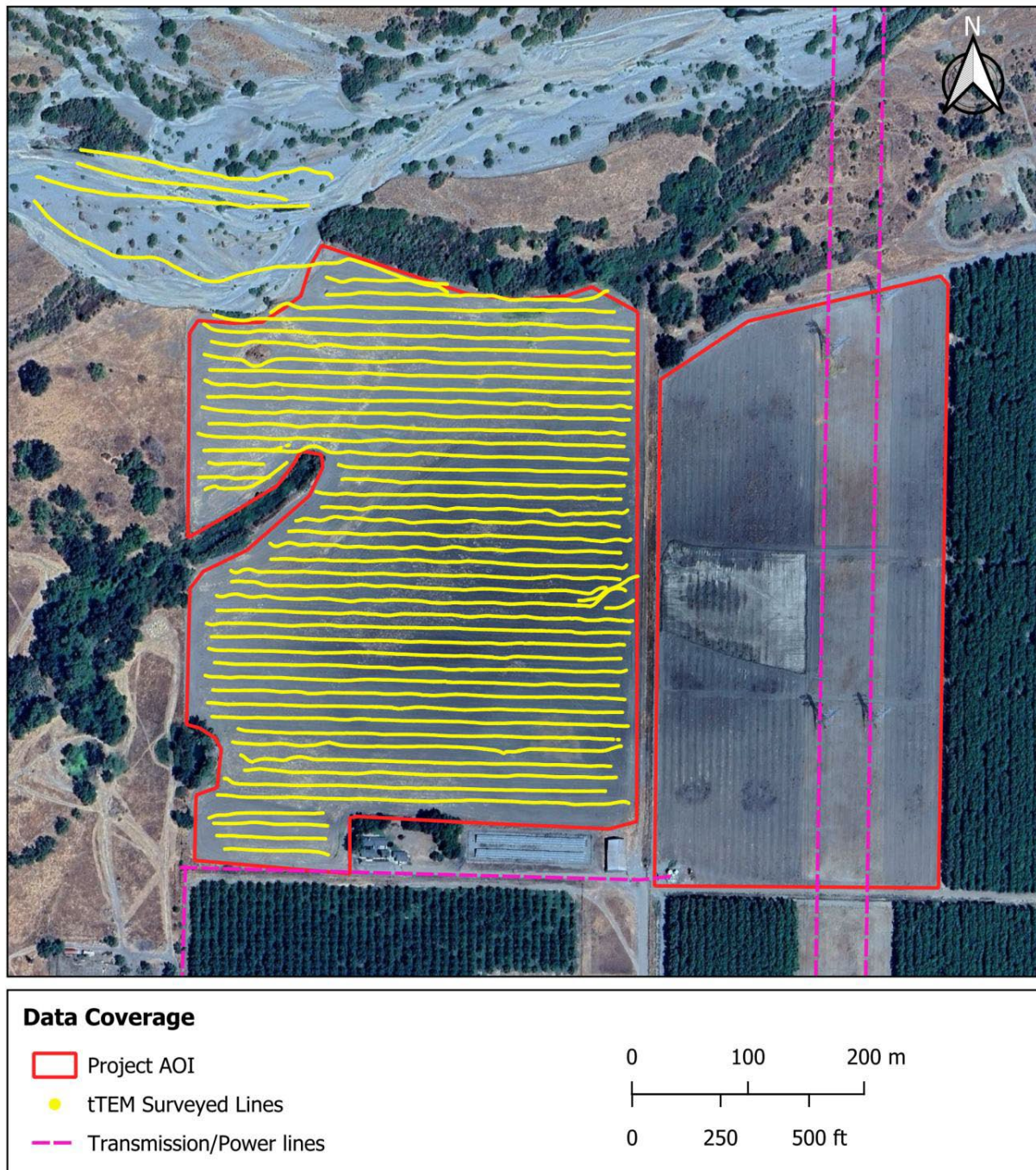


Figure 4-1. tTEM Survey Lines (from Geophysical Imaging Partners)

4.2. Data Analysis

Data collected during the survey were processed by Geophysical Imaging Partners following collection on the site. Resistivity data collected across the site was processed using software and manual review to remove noisy and erroneous data. Resistivity values are measured in ohm-m and correspond with various

particle sizes. Values around 10 ohm-m generally correspond to clays with particle sizes increasing up to about 100 ohm-m, which corresponds with coarse sands and gravels. The data were then organized and visualized utilizing the color scale shown in **Figure 4-2**. Data were then presented in two ways: a series of mean resistivity plan-view maps for various depth intervals, and a series of vertical sections covering the site which can be viewed in three dimensions. A detailed description the data processing steps can be found in the Data Processing and Inversion and Quality Control sections of **Appendix A: tTEM Geophysical surveys Esteve Property, Corning, California**.

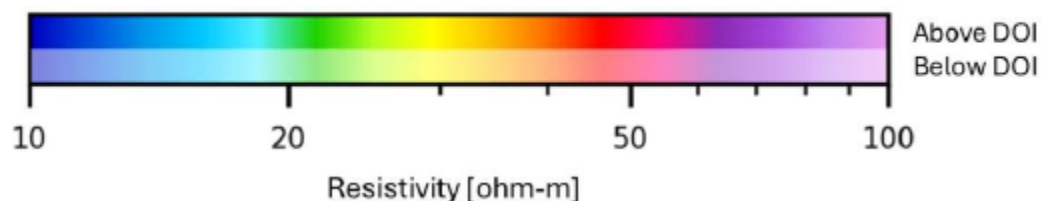


Figure 4-2. Scale Used to Represent Resistivity Values in Report (from Geophysical Imaging Partners, DOI refers to Depth of Investigation)

4.3. Results

Resistivity values across the site ranged from about 10 ohm-m to about 100 ohm-m. With 10 ohm-m values representing the finest grained materials and 100 ohm-m values representing the most coarse grained materials. Generally, resistivity values were highest in the northern portion of the site (nearest Thames Creek) from the surface down to about 30m (~100ft). This indicates that materials are generally more coarse grained in that area. At depths between 30m and 50m (100ft and 165ft) the coarsest grained materials are generally seen in the more central area of the site. Finally, at depths greater than 50m (165ft), the coarsest materials are seen in the southern portion of the site. See **Figure 4-3** for the mean resistivity plan-view map series. Water applied during groundwater recharge follows preferential paths through the most coarse-grained materials, either laterally or vertically. Thus, the pattern of resistivity observed in the data indicates that water applied to the surface of the site will rapidly infiltrate downwards to a depth of about 30m (150ft), then more slowly downwards and to the south at depths greater than 30m (150ft). This indicates that water applied at the site will flow away from Thames Creek at depth and will likely eventually enter the deeper portions of the aquifer.

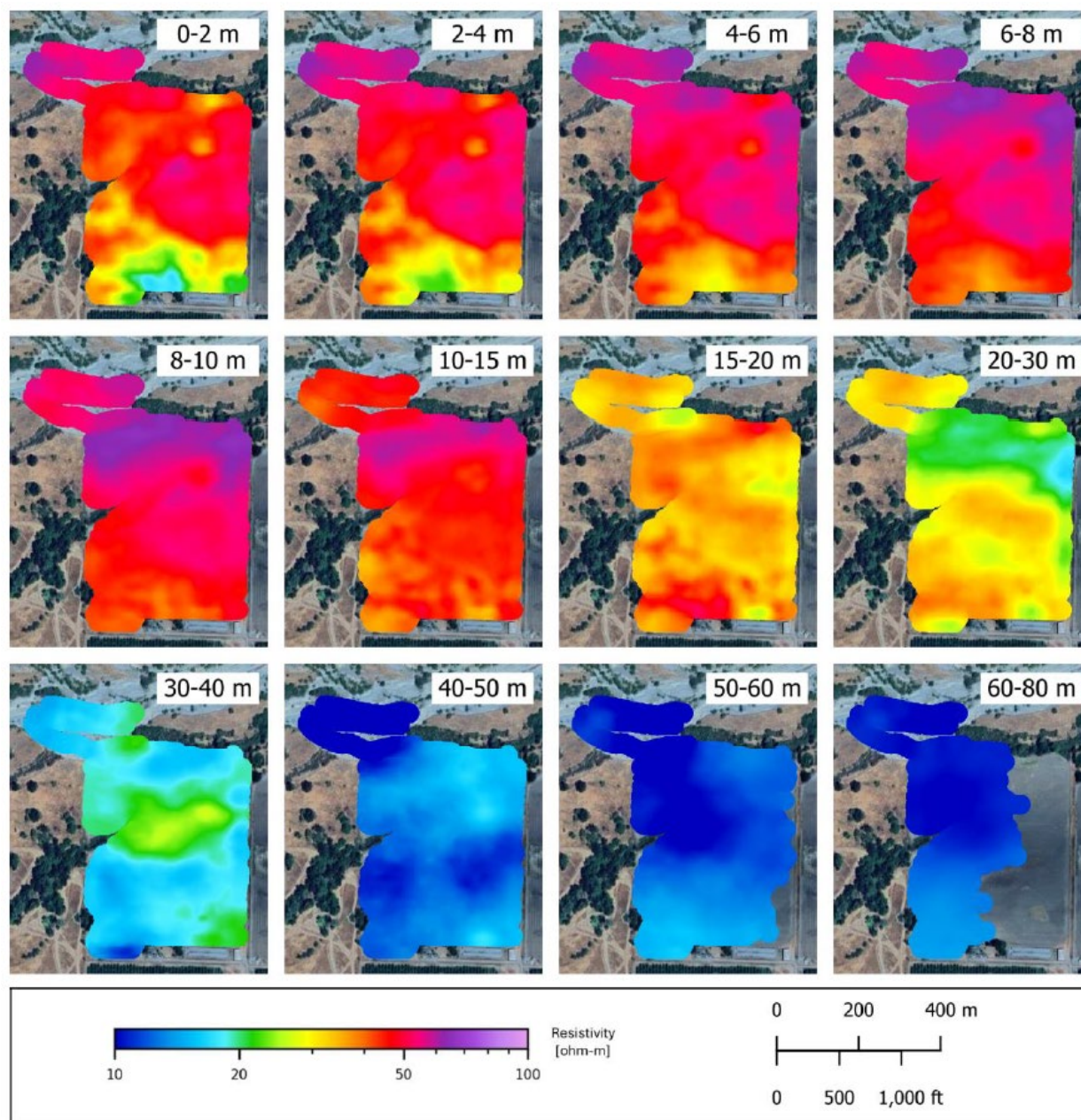


Figure 4-3 Mean Resistivity Plan-view Map Series (from Geophysical Imaging Partners)

5. CONCLUSIONS AND RECOMMENDATIONS

5.1. Conclusions

The pilot groundwater recharge tests aimed to evaluate the feasibility of using this site for efficient infiltration and to assess potential multi-benefit outcomes, including support for wildlife habitats. Additionally, the geophysical study attempted to identify possible subsurface flow paths of applied surface water. The results yielded the following conclusions:

- The location demonstrates an infiltration rate of 1.0 to 1.5 feet/day under saturated conditions, indicating high potential for groundwater recharge.
- Proximity to the Corning Water District distribution infrastructure ensures easy access to surface water, enhancing the site's viability for recharge operations.
- Recharge basins observed during the pilot tests supported various wildlife species, highlighting the site's potential for multi-benefit applications.
- Pilot Test #2, conducted over a longer duration, allowed for plant growth that further attracted numerous bird species, underscoring the ecological benefits of sustained recharge efforts (**Appendix B: Vegetation and Wildlife Photos**).
- The geophysical study indicates that applied water can rapidly infiltrate the subsurface to a depth of about 30m (150ft). Following that largely vertical infiltration, water will continue to slowly move downwards and to the south and make its way to deeper portions aquifer.

5.2. Recommendations

The following recommendations build on these key findings and guide future implementation:

- Landowner engagement for long term recharge: landowner feedback from the studies has been favorable. Further landowner engagement can help identify any obstacles to establishing a long-term recharge site.
- Establish funding for water: funding for purchases of water from CWD for recharge is crucial in converting this pilot site into a long-term recharge site. Establishing a source of funding for water would secure recharge benefits in the long term. Alternatively, this site could also be operated for recharge purposes via diversions from Thomes Creek under a temporary or permanent appropriative water right.
- Create infrastructure: improvements to the site including site leveling and larger, more substantial, berms around the infiltration area would increase the area available to apply water. This would allow more rapid infiltration of applied water, more total water infiltrated, or both.
- Assess monitoring options: The analysis in pilot test #2 was conducted using satellite imagery data. This methodology can continue to be employed to assess recharge amounts. In the future, existing nearby wells or dedicated monitoring wells should also be explored to help quantify benefits to water levels in the subbasin.

Appendix A: tTEM Geophysical surveys

Esteve Property, Corning, California

Project Report

tTEM Geophysical surveys Esteve Property, Corning, California



March 2025

Client:

Luhdorff & Scalmanini, Consulting Engineers
Woodland, CA

Att. Mr. Eddy Teasdale, Mr. William Anderson

Project #	25003
Project Name	tTEM geophysical surveys at Esteve Property, Corning, California
Date	26 March 2025
Client	Luhdorff & Scalmanini, Consulting Engineers
Prepared by	Ahmad-Ali Behroozmand and Max Halkjaer
Project description	tTEM geophysical surveys to enhance the understanding of the variations in the near-surface sediments at a potential recharge site near Corning, California, to support the client's ongoing managed aquifer recharge investigations.
Cover Photo	The tTEM system in operation within the study area.

Geophysical Imaging Partners, Inc.

Pleasant Hill, CA 94523, USA

Email: ahmad@geophysicalimaging.com, max@geophysicalimaging.com

Phone: +1 415-430-7173

March 26, 2025

Mr. Eddy Teasdale, Mr. William Anderson
500 First Street
Woodland,
CA 95695
USA



Geophysical Imaging Partners, Inc.
Pleasant Hill
California 94523

tTEM geophysical surveys near Corning, California

Dear Eddy and William,

We are pleased to submit this project report detailing the results of the geophysical investigations conducted at Esteve property, near Corning, California.

This project was conducted in the study area with the main objective of improving the understanding of the variations in the geological sediment in support of the client's ongoing managed aquifer recharge investigations.

It has been a pleasure to work with you on this project. We remain available to discuss this report or to answer any questions you may have.

Yours Sincerely,

A handwritten signature in black ink, appearing to read "A. Behroozmand".

Ahmad-Ali Behroozmand, PGp, PhD
Senior Geophysicist
ahmad@geophysicalimaging.com

A handwritten signature in blue ink, appearing to read "Max Halkjaer".

Max Halkjaer, M.Sc.
Principal Geophysicist/Hydrogeologist
max@geophysicalimaging.com

Table of Contents

Table of Contents	1
List of Figures	1
List of Appendices	2
Abbreviations.....	3
Introduction	4
Field Operations.....	6
Data Collection.....	8
Instrument Issues.....	8
Weather	8
Data Processing and Inversion	10
tTEM Data Processing Steps.....	10
tTEM Data Inversion Steps	11
Quality Control.....	11
Results	12
Color scale.....	13
Mean resistivity plan-view maps.....	13
Vertical sections	14
Data Deliverables	17
Conclusions	17

List of Figures

Figure 1 Overview map of the tTEM surveyed area. Yellow lines show tTEM surveyed lines. The eastern field was not surveyed due to a transmission line crossing the field, which interferes with the TEM data.	5
Figure 2 The tTEM system assembled and tested before starting the survey in the morning of January 16, 2025.....	6
Figure 3 The transmitter loop (red wire) attached to a frame with red arms that is mounted on a sled (black). Similarly, the receiver coil (white box) is mounted on a sled and pulled behind the transmitter loop.....	7
Figure 4 The tTEM system in operation in the riverbed.	9
Figure 5 <i>General correlation between resistivity, type of geologic materials, and water quality.</i>	13
Figure 6 Resistivity color scale used for all presentations in this report. DOI refers to depth of investigation.....	13
Figure 7 Mean resistivity maps for depth intervals from the terrain to 100 m (328 ft).	15

Figure 8 An example of a vertical model section from the study area.	16
---	----

List of Appendices

Appendix 1 – TEM Theory

Appendix 2 – tTEM Instrumentation, Processing & Inversion Settings

Appendix 3 – Quality Control Maps

Appendix 4 – Mean Resistivity Maps

Appendix 5 – Vertical Section

Appendix 6 – A description of the digital data formats

Abbreviations

1D	One Dimensional
AMSL	Above Mean Sea Level
ATV	All-Terrain Vehicle
BGS	Below Ground Surface
DC	Direct Current
DEM	Digital Elevation Model
DOI	Depth of Investigation
EM	Electromagnetics
EPSCG	European Petroleum Survey Group
Ft	Foot
GERDA	Geophysical Relationship Database
GPS	Global Positioning System
HM	High Moment
LCI	Laterally Constrained Inversion
LM	Low Moment
M	Meter
MAR	Managed Aquifer Recharge
OHM-M	Ohm Meter
QC	Quality Control
SCI	Spatially Constraint Inversion
TEM	Transient Electromagnetics
tTEM	Towed TEM

Introduction

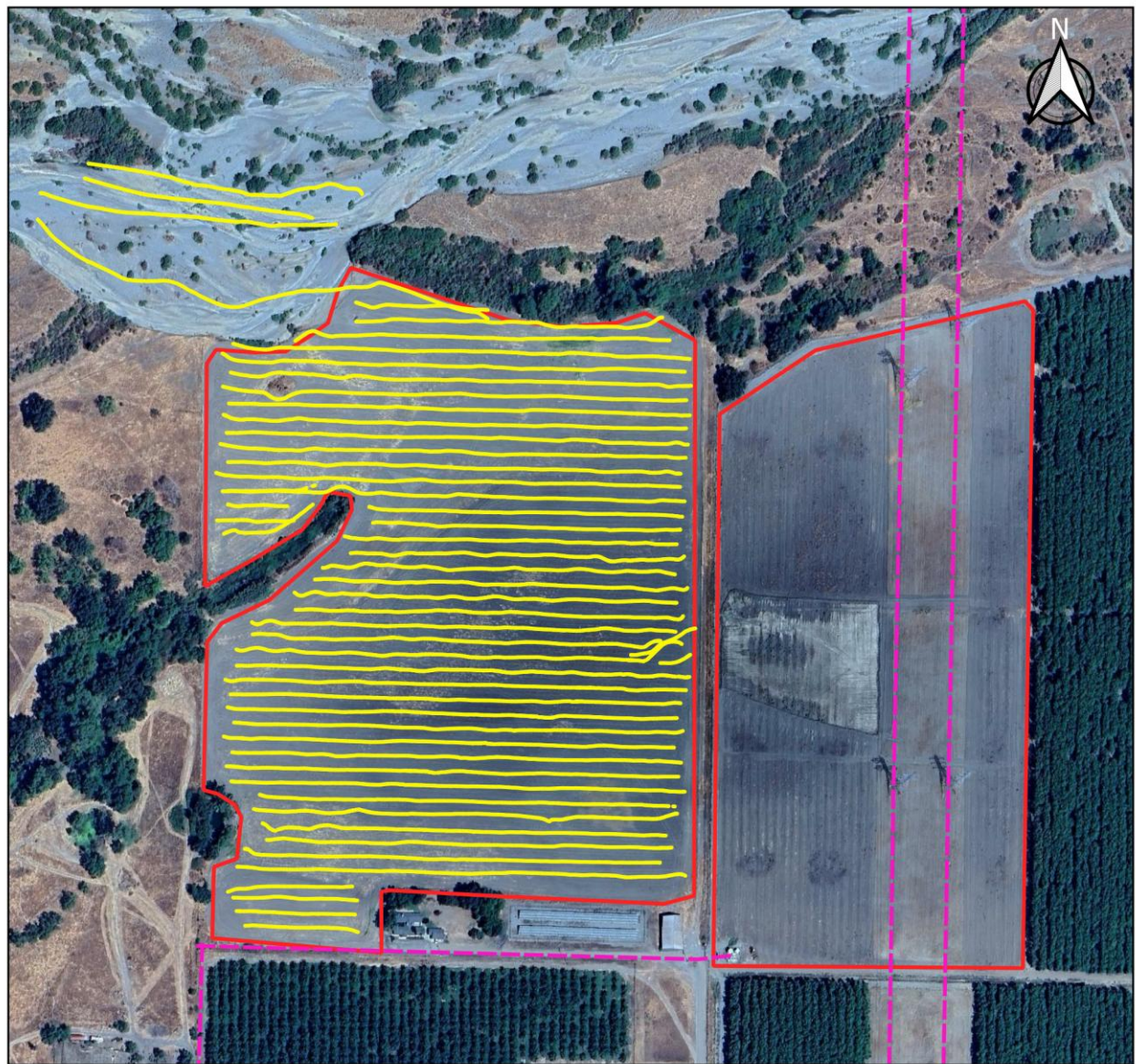
Geophysical Imaging Partners, Inc. (GIP) conducted a towed Transient Electromagnetic (tTEM) survey at Esteve property near the city of Corning, California. The purpose of this geophysical investigation was to further understand and characterize subsurface sediments and geology to support the client's ongoing managed aquifer recharge (MAR) investigations.

One (1) day of tTEM geophysical investigations were conducted within the study area proposed by the client. A location map of the surveyed area is shown in Figure 1. Of the two adjacent proposed fields, the eastern field was not surveyed due to a transmission line crossing the field, which would interfere with the TEM data.

Following data processing, the tTEM data were interpreted as smooth (multi-layer) electrical resistivity models through geophysical inversions. The tTEM results provide a detailed representation of electrical resistivity variations along the survey lines. The results are presented in the form of mean resistivity plan-view maps and vertical resistivity cross-sections. The tTEM depth of investigation (DOI) varies across the study area, between 45 m (148 ft) and greater than 70 m (230 ft) below ground surface (bgs).

This report provides a summary of the field operations and a description of the tTEM results. In addition, the following appendices provide supplementary information:

- Appendix 1: General introduction to the TEM method,
- Appendix 2: tTEM system specifications, including system configuration and details about processing and inversion settings,
- Appendix 3: QC parameters,
- Appendix 4: Mean resistivity plan-view maps at different depth intervals across the study area,
- Appendix 5: Cross sectional illustrations of the results.
- Appendix 6: A description of digital data formats.



Data Coverage

- Project AOI
- tTEM Surveyed Lines
- Transmission/Power lines

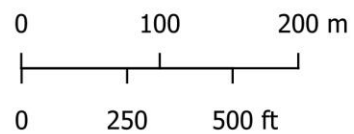


Figure 1 Overview map of the tTEM surveyed area. Yellow lines show tTEM surveyed lines. The eastern field was not surveyed due to a transmission line crossing the field, which interferes with the TEM data.



Figure 2 The tTEM system assembled and tested before starting the survey in the morning of January 16, 2025.

Field Operations

The fieldwork took place on January 16, 2025, conducted by Max Halkjaer and Ahmad-Ali Behroozmand of Geophysical Imaging Partners. The equipment was transported to and from the site using a cargo van. The system was assembled onsite, and test measurements were performed before starting the survey.

The transmitter and receiver units were mounted on sleds and towed behind an all-terrain vehicle (ATV). The sleds and frames are made from nonmetallic materials to prevent noise interference with the data (Figure 3). All electronic instruments and the power supply were mounted in the back of the ATV.

The tTEM system was checked and tested prior to the fieldwork to ensure its proper functionality. The TEM measurements, referred to as “soundings”, provide subsurface information to depths greater than 70 m (230 ft). The depth of investigation varies depending on subsurface conditions and the signal-to-noise ratio at each site.

The tTEM data characterizes the electrical resistivity of subsurface materials by injecting a direct current (DC) into the transmitter loop, emitting magnetic fields into the ground. After the current stabilizes, it is abruptly turned off. This abrupt turnoff of the transmitter current induces short-duration eddy currents in the ground, which propagates downwards and outwards. A receiver coil located on a sled behind the transmitter loop then measures the decaying magnetic field resulting from the eddy currents.

For further details about the TEM method and the tTEM system specifications, please see Appendix 1 and Appendix 2.



Figure 3 The transmitter loop (red wire) attached to a frame with red arms that is mounted on a sled (black). Similarly, the receiver coil (white box) is mounted on a sled and pulled behind the transmitter loop.

Data Collection

Data was collected along WE-oriented lines with a 30 m line spacing. The dense line spacing provided detailed 3D mapping of the subsurface. The survey lines were monitored on the tTEM navigation system. This allowed real-time tracking of the lines and consistent spacing between neighboring lines. The system's functionality was frequently monitored by the operator through the navigation system to ensure all measuring parameters remained within expected ranges.

Overall, the site conditions were well-suited for acquiring tTEM data. As anticipated, data collected near electromagnetic noise sources, such as powerlines, fences, and other metal objects, were affected by interference. These data were removed during the processing step (see Appendix 3).

Instrument Issues

No instrumental issues were encountered during the survey.

Weather

The weather during the survey was sunny and pleasant, with temperatures reaching ~ 65F.



Figure 4 The tTEM system in operation in the riverbed.

Data Processing and Inversion

The processing and inversion of the tTEM data were carried out with the software package Aarhus Workbench (<https://www.aarhusgeosoftware.dk/aarhus-workbench>). We utilized applications that are specifically designed for processing and inversion of tTEM data.

During data processing, noisy data are removed, and the remaining data are averaged. Then the voltage data are fitted by identifying a geophysical resistivity model that best matches the measured data. The results are resistivity models presented as depth slices across the area and as vertical cross sections.

tTEM Data Processing Steps

The raw data collected from the instrument underwent quality control. Then the dataset was processed to remove unusable, noisy data. The tTEM data was processed with the following steps:

1. Data were imported into a [Firebird](#) database.
2. Line numbers were assigned to the data during the field operation. The assigned line numbers were reviewed and updated.
3. Verification that all EM data and secondary data (GPS, speed, transmitter currents, etc.) were continuously measured throughout the survey.
4. Data were checked to ensure proper masking at turning points to avoid data where the system was not properly aligned.
5. Secondary data were reviewed to ensure they met specifications and do not vary significantly along the survey lines.
6. Processing of GPS data.
7. A standard uniform 3% noise was assigned to all data.
8. A standard processing scheme was defined to automatically reject data and assign noise.
9. Manual inspection of each survey line. Data determined noisy, which had not been rejected in the previous step, were removed. Noise sources include overhead powerlines, buried power cables, metal fences, and other man-made sources. This was done for the individual measurements (soundings) and for sequences of soundings along the survey line.
10. Data recorded while the system was stationary was removed manually.
11. Elevation values were assigned to each data point from a digital elevation model grid to improve elevation accuracy of the resulting models. A USGS DEM layer ([3D Elevation Program; 3DEP](#)) with grid spacings of 1/3 arc-seconds (~ 10 m / 33 ft) was used for this study.
12. Data were averaged along the lines using a trapezoidal filter. This step involved averaging more data from late time gates compared to fewer data from early time gates. The aim was to improve the signal-to-noise ratio for data representing the deeper parts while maintaining high resolution information for near-surface features along the lines.
13. A final processed dataset with a sounding distance of approximately 10 m (33 ft) was developed.

More information about the tTEM data processing can be found in Appendix 2.

tTEM Data Inversion Steps

After processing the data, an inversion algorithm was applied to the entire dataset to estimate subsurface electrical resistivity models. The following inversion scheme was used:

1. Define the number of model layers and layer thicknesses and set horizontal and vertical constraints on resistivities.
2. Perform inversion using the laterally-constrained inversion (LCI) approach ([Auken et al., 2005](#)) and the spatially-constraint inversion (SCI) approach ([Viezzoli et al., 2009](#)). The LCI inversion results were used for an initial assessment of the estimated resistivity models and to identify if any parts of the dataset required additional processing before running the SCI inversion.
3. Present the data as depth slices. If the depth slices revealed distinct anomalies, the processing of the corresponding data was revisited, and the data were re-inverted.
4. Calculate the depth of investigation (DOI) for each resistivity model through sensitivity analysis.

More information about the inversion process can be found in Appendix 2.

Quality Control

Quality control (QC) was performed during data acquisition in the field, in the office on the same day the data was collected, and as part of the data processing and inversion.

QC in the field

Throughout data acquisition, the system components were frequently assessed to ensure that all parts were intact and secure. In addition, the TEM signal, battery voltage, current, temperature and GPS reception were constantly monitored.

Overall, good signal-to-noise ratios (SNR) were observed across the surveyed area. Data collected on the eastern side of the field were noisier due to proximity to the transmission line and a fence separating the two fields.

Daily QC at the Office

At the end of the survey day, the data was exported from the instrument and imported into the processing and inversion software. The TEM data files were checked for completeness and the GPS data were checked for accuracy.

QC of the Processed and Inverted Data

The processed and inverted data were quality controlled by inspecting various parameters like the number of data points per location, the last data point at each location, noise levels, data fits etc. Three types of thematic maps are presented in Appendix 3: Accepted versus rejected data, Data residual, and Depth of investigation.

Accepted and Rejected Data

The data coverage map shows the location of the tTEM data accepted for inversion and the data that were rejected. Data were rejected near the ends of lines due to the ATV-sensor setup turns and near powerlines and man-made installations due to noise. Overall, the survey site provided favorable conditions for data collection.

Since the survey lines were planned to minimize the amount of data recorded too close to powerlines and fences, and the area of interest consists of open fields, only a relatively small number of data points were removed. During data processing, the raw data were reviewed prior to averaging, and noisy data close to man-made installations were removed. After the first inversion, additional data points recorded too close to man-made installations were identified and removed.

Depth of investigation

The depth of investigation (DOI) indicates the depth to which the resulting model can be considered reliable. DOI varies based on geological and hydrogeological conditions, electromagnetic noise level, and system specifications. In general, DOI is larger in resistive ground and smaller in conductive ground. In addition, it increases by increasing the induced signal, achieved by injecting higher current, increasing the size of the transmitter loop, or increased decay curve averaging (stack size).

Across the survey area, the DOI was calculated for each model. On vertical sections (Appendix 5), depths beyond the DOI are shown with fading colors. On plan-view maps (Appendix 4), resistivities below the calculated DOI are masked. In Appendix 3, the tTEM DOI across the study area is shown, extending to more than 70 m (230 ft) below the ground surface (bgs). In general, the DOI ranges between ~ 45-75 m (148-246 ft).

The DOI is shallower in the eastern part of the field due to reduced data quality.

Data residual

Appendix 3 presents a location map of data residual values across each survey site. Data residual, or data fit, was used to assess the inversion results. A residual of 1 or lower indicates that data was fitted within the assigned uncertainties. In this survey, residual values were mostly below 0.5, which indicates a very good data fit.

Results

As previously described, the measured data are modeled to represent electrical resistivities at various depths, which can then be interpreted as lithology to gain insight into the site's geology. The tTEM results are presented as vertical resistivity sections and mean resistivity plan-view depth maps.

Color scale

The tTEM method measures the electrical resistivity of the subsurface. To obtain the subsurface lithologic information, the measured electrical resistivities must be transformed into lithologies. Transforming resistivity to lithology is based on a general correlation between resistivity and sediment type. Figure 5 shows a general correlation, where low permeability clay has a low resistivity value, sandy clay typically has a medium-range resistivity value, and sand to coarse sand has a relatively large resistivity value. This correlation is a general assumption and the range of resistivity for each lithologic unit can vary between locations. The water quality and saturation degree can also impact the resistivity, i.e., the more saline the water, the lower the formation resistivity and the lower the saturation degree, the higher the formation resistivity. Therefore, correlation with additional data sources if available (such as information from boreholes and water quality) and general geologic knowledge of the study area are crucial to obtain the most accurate description of the subsurface hydrogeology.

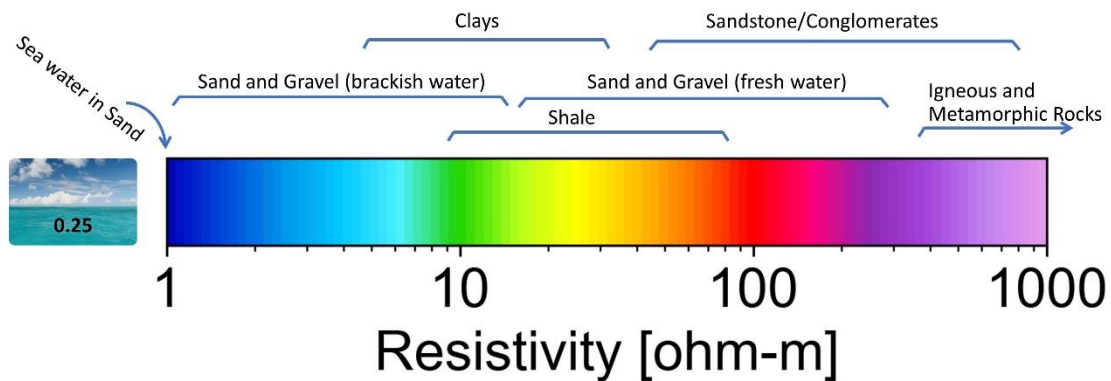


Figure 5 General correlation between resistivity, type of geologic materials, and water quality.

In this project, the resistivity colormap was adjusted to enhance the visualization of the resistivity variations across the study area. The color scale used for all presentations in this report is shown in Figure 6.

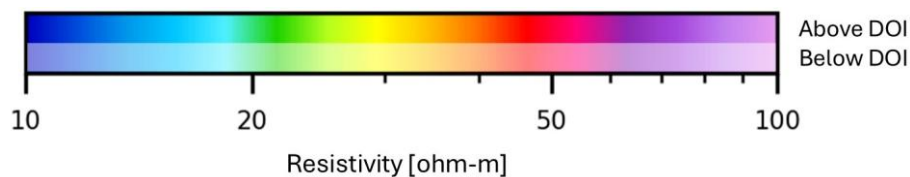


Figure 6 Resistivity color scale used for all presentations in this report. DOI refers to depth of investigation.

Mean resistivity plan-view maps

Mean resistivities are presented as plan-view maps at various depth intervals. The maps show resistivity averages over 2-m (7-ft), 5-m (16-ft), 10-m (33-ft), and 20-m (66-ft) depth intervals. An overview of the

mean resistivity maps, ranging from the ground surface to a depth of 80 m (262 ft), is shown in Figure 7. These illustrations are meant to provide a quick overview of the variations within the field.

In Appendix 4, the mean resistivity maps are scaled up in size and cover the entire depth range. The mean resistivity maps provide insights into variations across the surveyed area at each depth interval.

Vertical sections

Figure 8 provides an example of a vertical resistivity model section from the study area, showing detailed structural variations along the section. In Appendix 5 several vertical sections are presented.

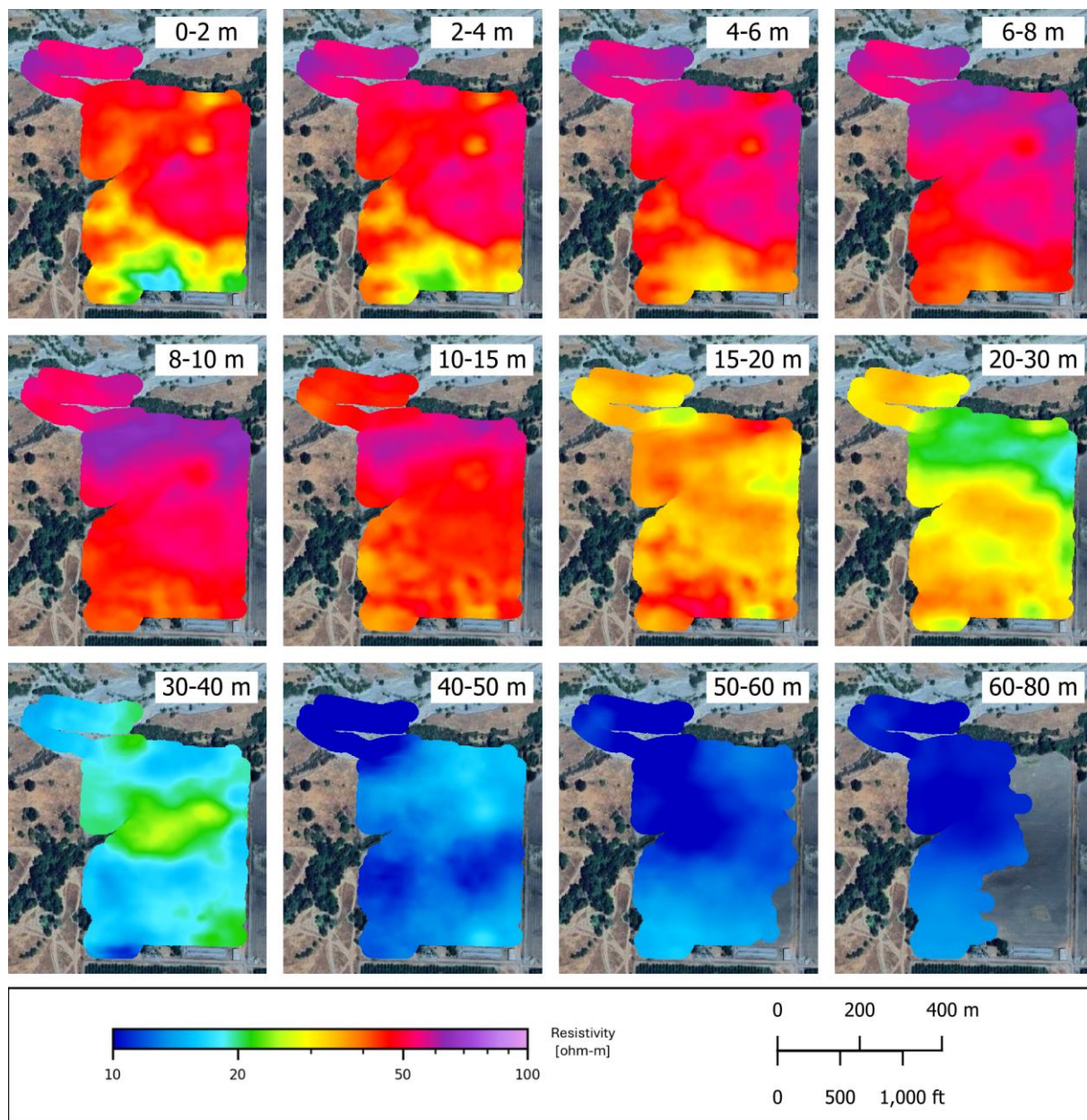


Figure 7 Mean resistivity maps for depth intervals from the terrain to 100 m (328 ft).

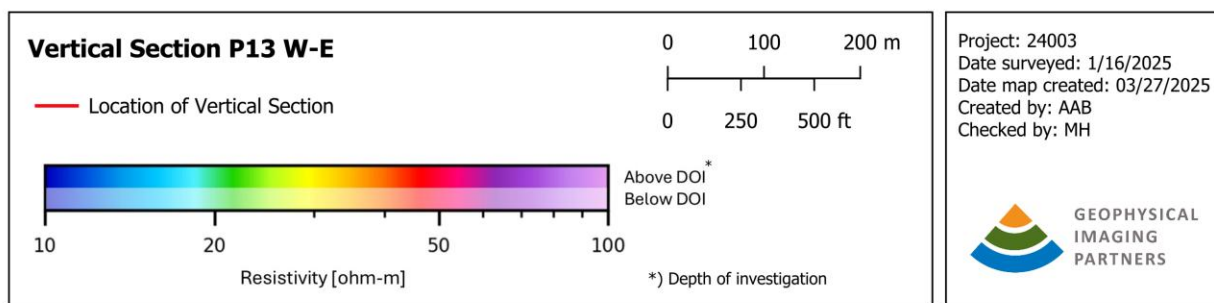
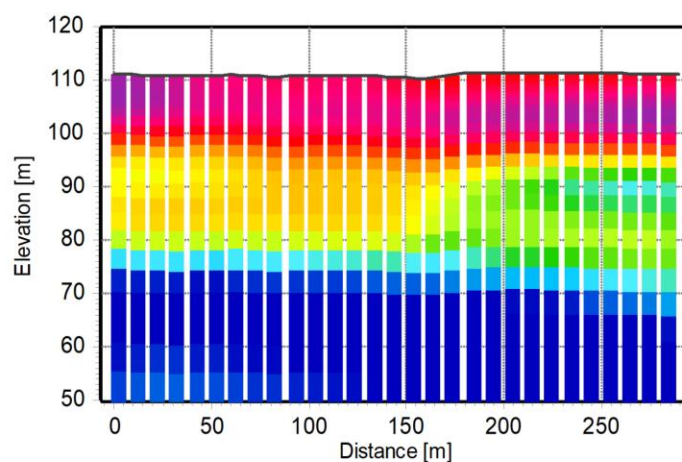


Figure 8 An example of a vertical model section from the study area.

Data Deliverables

The following files have been provided as project deliverables. Each set of files is accompanied by a readme.txt file describing the file formats and contents.

1. Raw data as extracted from the instrument, including:
 - A. Ascii files with information about the geographical coordinates, transmitted current and many other supporting data. All files are named YYYY_MMDD_HHMMSS followed by three letters as an extension.
 - B. A file with a filename extension LIN describes the start and end of each survey line.
 - C. Binary data files with the electromagnetic decay measurements. These files have a filename extension STB. The top section of the binary file is an ascii section with all information about measurement cycles and settings in the instrument.
2. A [Firebird](#) database (in the [GERDA](#) format) containing all collected data, processed data, as well as the inverted model results.
3. ArcGIS layers including:
 - A. *Layout*. ArcGIS shape files (*.shp) containing general information about the surveyed area (project area outline etc.), location of tTEM survey lines day and locations of the remaining data after processing.
 - B. *Mean Resistivity Maps*. Geo-referenced TIF files (*.tif*) illustrating plan-view maps of average resistivities within different depth intervals that are presented in this report. Each file name includes information about the top and bottom of the interval.
 - C. *Model Sections*. ArcGIS shape files (*.shp) containing locational information for the vertical sections presented in this report.
4. Model outputs. Ascii files (with a filename extension XYZ) containing exported models from the Firebird database in different file formats.
5. Google Earth KMZ files, which include the mean resistivity maps and model sections, among others.
6. A project report, delivered as a PDF file.

Conclusions

The tTEM survey provided high-quality data, enabling continuous mapping of geologic units and detailed information about their characteristics, including heterogeneity, continuity, and extent of each unit. In addition, the results provide insight into the suitability of the study area for managed aquifer recharge.

This section provides general conclusions and an overall interpretation of the results in terms of the structures observed in the geophysical data.

The data quality is high. Overall, the top 15 m is resistive, which suggests favorable conditions for recharge. Resistivity values are generally higher in the northern part of the site. In the top 4-m, resistivities are lower in the southern part, which may indicate finer materials (see Figure 7). From approximately 15 m, resistivity values start to decrease. Below 40 m, resistivities are below 20 ohm-m with varying resistivities across the site. This suggests the presence of brackish water and/or fine-grained materials.

The depth of investigation (DOI) is shallower in the eastern part of the site due to interference from a fence and the transmission line, which affected late-time data.

Given the overall homogeneity of the top resistive layer, it is likely that the adjacent field to the east is also favorable for recharge. However, this should be validated with other types of geophysical data (e.g., electrical resistivity tomography) or borehole data.

Appendix 1 – TEM Theory

For decades electromagnetic (EM) methods have been used worldwide for cost effective mapping of the subsurface materials for different applications. More recently, the accuracy of the instruments and their ability to obtain information about aquifers and hydrogeological properties has improved significantly. As a result, the TEM method is now one of the most efficient geophysical technologies for groundwater investigations.

Principles of TEM

The physical principle of the TEM is based on the electromagnetic induction phenomenon. The ground is first energized by a primary magnetic field generated by a direct current injected in a transmitter (Tx) loop. When the current stabilizes, the transmitter is turned off abruptly. During this rapid decay of the current an electromotive force results in short-duration eddy currents whose strength is largest in conductive parts of the ground. The EM induction phenomenon generates what is called the secondary magnetic field, the decay of which is measured just after the end of the turn-off using an induction receiver coil located in the center of the Tx loop (central loop configuration like ground-based stationary TEM) or outside the Tx loop (off-set configuration like tTEM). The actual measurement, referred to as TEM “sounding” or dB/dt curve, is the time derivative of the magnetic flux passing through the receiver coil. An example of a measured sounding curve is shown in Figure A1- 1.

The TEM response is measured and interpreted as a function of time. Just after the current in the Tx loop is turned off, the eddy currents in the ground will be close to the surface, and the measured signal primarily reflects the resistivity of the top layers. At later times the current will run deeper in the ground, and the measured signal contains information about the resistivity of the deeper layers. This is why the method is referred to as time-domain EM or TEM. Measuring a TEM sounding will therefore provide information about the resistivity as a function of depth.

The transmitter magnetic moment (Tx loop area x current x number of wire turns) and the signal-to-noise ratio (SNR) determine the depth of investigation (DOI). A stronger magnetic moment enables deeper penetration of the magnetic fields and thus greater DOI. The SNR depends on the ground electrical resistivity and ambient noise. The higher the SNR, the greater the DOI.

More information about the principles of the TEM method can be found in Ward and Hohmann (1988).

Noise in TEM data

TEM data are comprised of different types of noise components. Noise can cause bias signals and affect the depth of investigation and if not properly identified and removed, can result in incorrect geological and hydrological interpretations. The different sources of noise include: (1) Galvanic coupling caused by the electromagnetic signal induced in a metal object, such as grounded overhead powerlines, metal pipes, metal fences etc., (2) Capacitive coupling caused by the induced EM signal in an insulated installation such as a power cable, (3) Coherent noise from electrical powerlines, (4) Atmospheric noise, and (5) Instrument internal noise.

References

Ward SH, Hohmann GW (1988) Electromagnetic theory for geophysical applications. In: Nabighian MN (ed) Electromagnetic methods in applied geophysics, vol 1. SEG, Tulsa, pp 131–311.

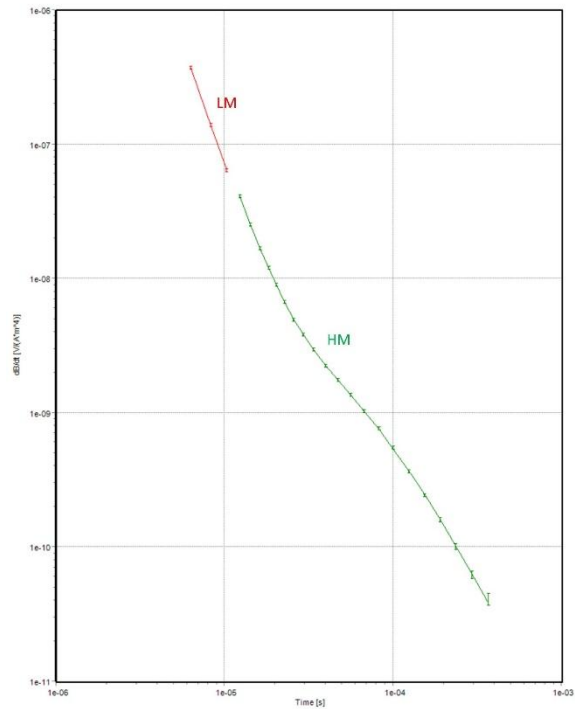


Figure A1- 1 An example of a $\frac{dB}{dt}$ curve (sounding data) measured with the tTEM system.

Appendix 2 – tTEM Instrumentation, Processing & Inversion Settings

This appendix describes the tTEM instrument setup, processing and inversion settings.

Instrument Setup

The tTEM instrument measures data continuously while being towed on the ground. The system is designed to provide very high near-surface resolutions using very early time gates. The tTEM data collection was performed using an offset loop configuration (Figure A2- 1), employing a 2.9 m x 2.9 m (9.5 ft x 9.5 ft) single-turn square-shaped transmitter loop and a 0.5 m x 0.5 m (1.6 ft x 1.6 ft) multi-turn receiver coil placed 7.5 m (25 ft) behind the transmitter loop. The transmitter loop was positioned 4 m (13 ft) away from the ATV. The entire system layout extended to 14.4 m (47 ft).

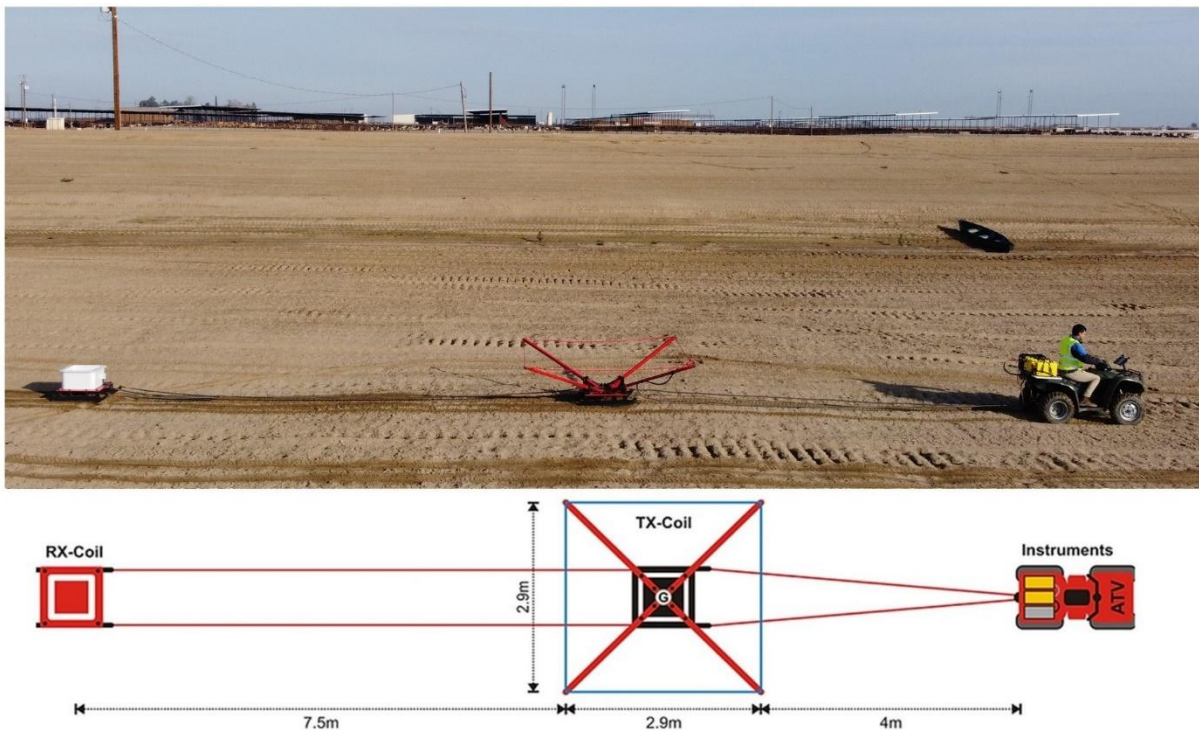


Figure A2- 1 The tTEM system configuration.

Instrument ID

The ID information of the instruments used in this survey can be found in Table A2- 1.

Unit	ID1	ID2
tTEM instrument		V100A240014
RC20 Receiver coil	RCS20-0012	V112A240012
tTEM Receiver Platform		20220850
tTEM Tx Coil	331	V106A240007

Table A2- 1a ID information for the instruments used in this survey.

Device positions and geometry

The positions and geometry of the main tTEM system components with respect to the transmitter frame are listed in Table A2- 2 in (x,y,z) coordinates. X and y define the horizontal plane. Z is perpendicular to (x, y). X is positive in the survey direction, y is positive to the right of the survey direction, and z is positive downwards.

Unit	X (m)	Y (m)	Z(m)
GP_Tx (GPS)	7.85	0.00	-0.90
RxZ (Z-receiver coil)	-9.28	0.00	-0.30
Tx-Coil, center	0.00	0.00	-0.97
Tx-Coil corner 1	-1.45	-1.45	-0.97
Tx-Coil corner 2	1.45	-1.45	-0.97
Tx-Coil corner 3	1.45	1.45	-0.97
Tx-Coil corner 4	-1.45	1.45	-0.97

Table A2- 2 Positions and geometry of the tTEM transmitter, receiver, and GPS units

Measurement cycle

The key parameters defining the transmitter setup are listed in Table A2- 3.

Parameter	LM	HM
Moment ID	2	1
No. of turns	1	1
Transmitter effective area (m2)	9 m2	9 m2
Tx Current	~ 3 A	~ 30 A
Tx Peak moment	~ 27 Am2	~ 270 Am2
Repetition frequency	2016 Hz	564 Hz
Raw Data Stack size	336	248
Period Time	496E-6	1773E-6 s
Raw Moment cycle time	0.17 s	0.50 s
Tx on-time	200 μ s	450 μ s
Duty cycle	40%	25%
Turn-off time	2.6 μ s at 3 Amp	4.2 μ s at 30 Amp
Number of gates	10	21
Gate time interval (gate center time)	4 μ s – 30 μ s	12 μ s – 910 μ s
Front-gate	2 μ s	4 μ s

Table A2- 3 Basic settings of the instrumentation.

Receiver coil

The receiver coil can be described by the following parameters. The parameters are used in the inversion scheme.

Parameter	Value
Low pass filter frequency	679 kHz
Low pass filter order	1
Effective area	20m ²

Table A2- 4 Receiver coil parameters.

Processing and inversion settings

The processing and inversion are based on the Aarhus Workbench software, version 6.9.0.0.

A 30-layer model has been applied. Table A2- 5 lists the fixed layer thicknesses, depth to bottom of layer and the initial resistivity assigned to the model layers. For this survey, an initial resistivity value of 40 ohm-m was assigned to all layers during the inversion.

Layer	Thickness [Meter]	Depth [Meter]	Start value [Ohm-m]
1	1	1	40
2	1.1	2.1	40
3	1.2	3.3	40
4	1.3	4.6	40
5	1.4	6	40
6	1.5	7.5	40
7	1.7	9.1	40
8	1.8	11	40
9	2	12.9	40
10	2.1	15.1	40
11	2.3	17.4	40
12	2.5	19.9	40
13	2.8	22.7	40
14	3	25.7	40
15	3.3	28.9	40
16	3.5	32.5	40
17	3.9	36.3	40
18	4.2	40.5	40
19	4.6	45.1	40
20	5	50.1	40
21	5.4	55.5	40
22	5.9	61.4	40
23	6.4	67.8	40
24	7	74.8	40
25	7.6	82.4	40
26	8.3	90.6	40
27	9	99.6	40
28	9.8	109.4	40
29	10.6	120	40
30	--		40

Table A2- 5 Depth discretization and starting resistivity values for the inversion.

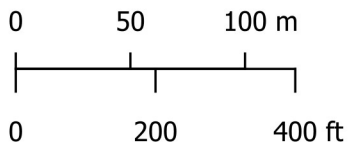
Appendix 3 – Quality Control Maps



Base Map: Google Satellite,
EPSG: 3310, NAD83 / California Albers

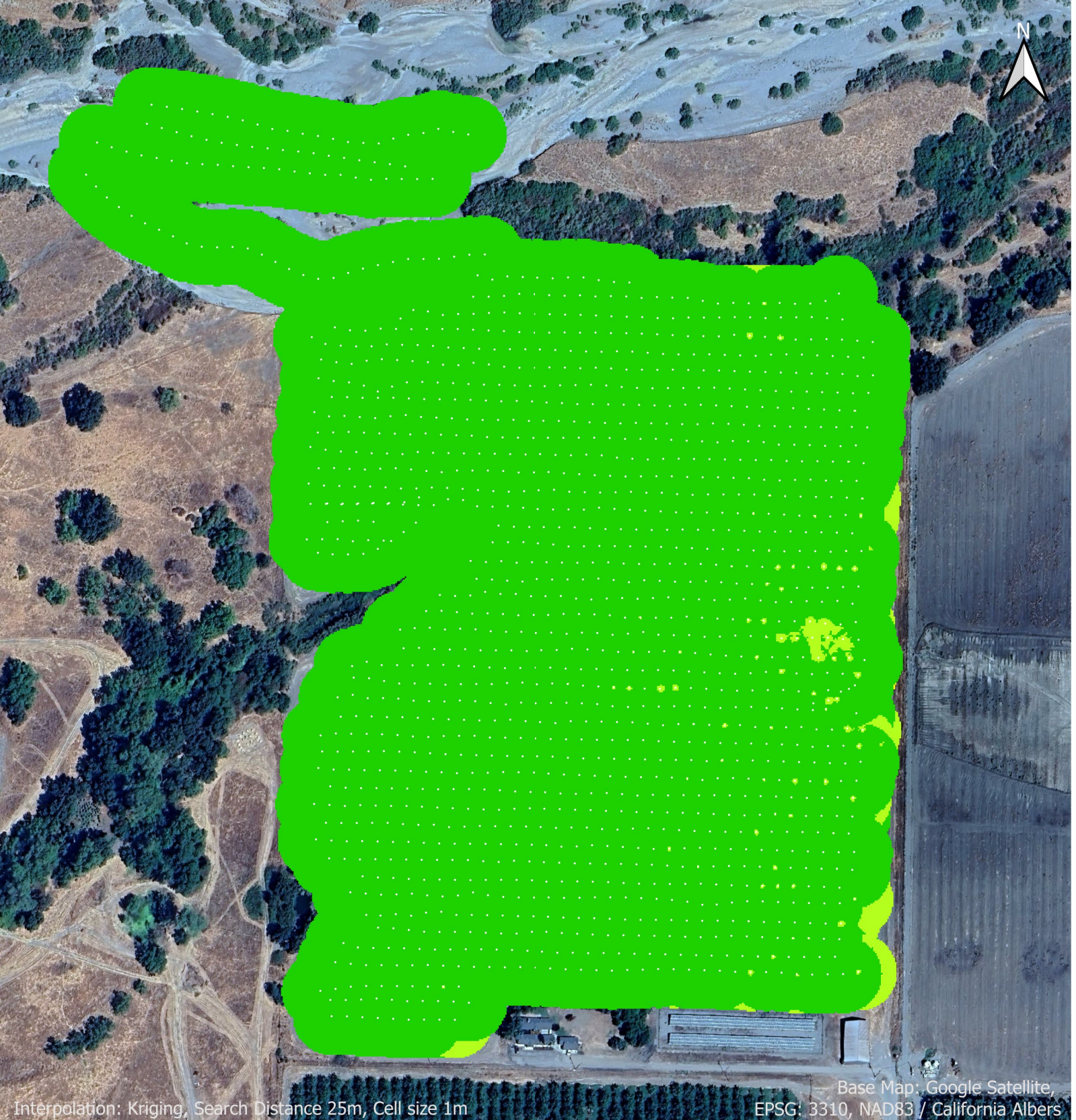
Data Coverage

Data used for inversion: Green dots
Rejected data: Red dots



Date surveyed: 1/16/2025
Date map created : 03/26/2025
Created by: AAB
Checked by: MH



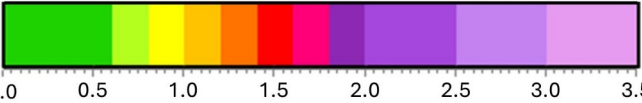
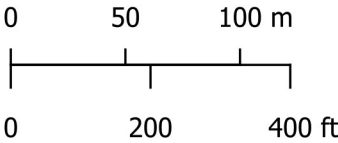


Interpolation: Kriging, Search Distance 25m, Cell size 1m

Base Map: Google Satellite,
EPSG: 3310, NAD83 / California Albers

Data Residual

Data Points: Gray dots

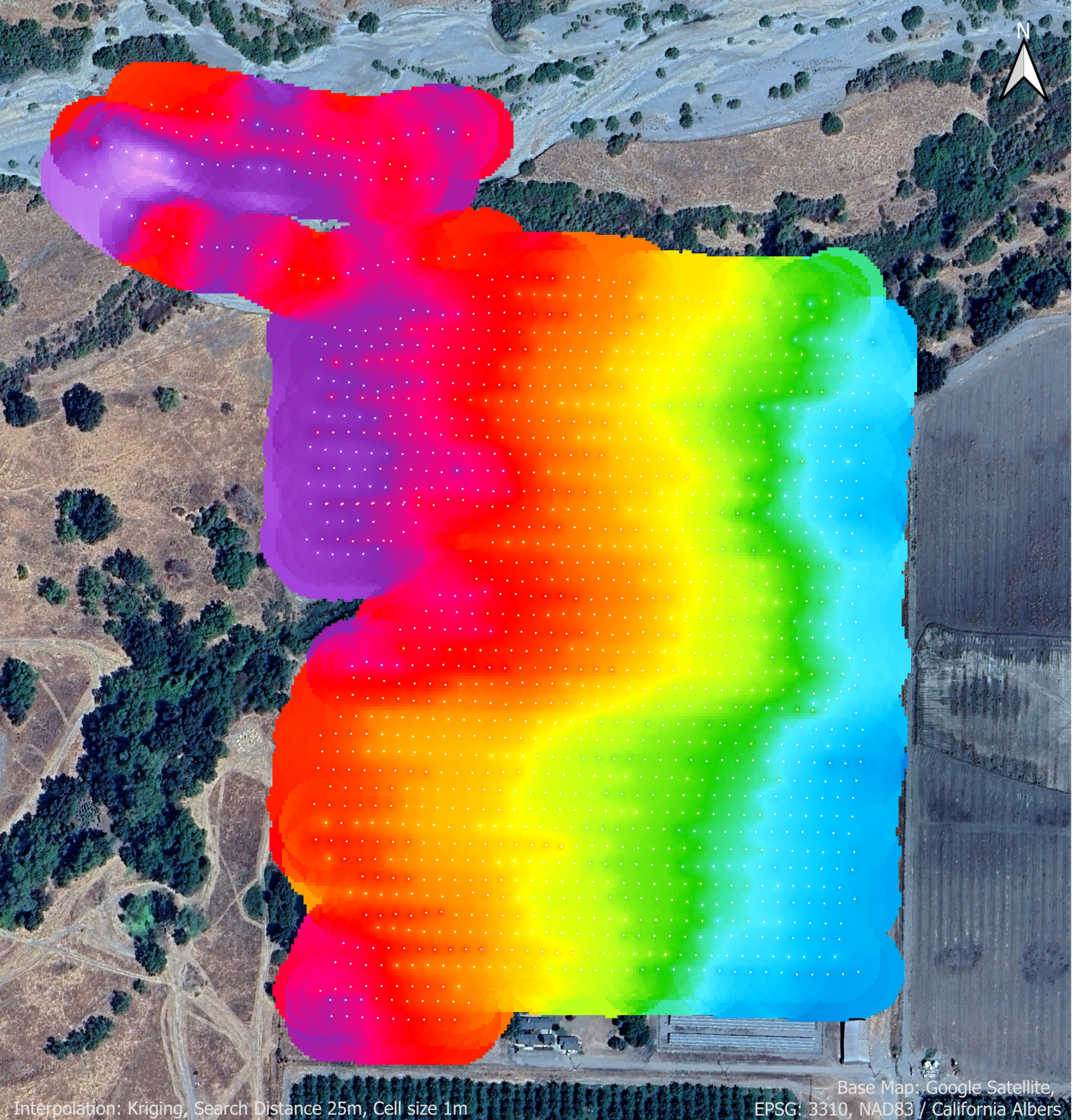


Residual
[-]

Date surveyed: 1/16/2025
Date map created : 03/26/2025
Created by: AAB
Checked by: MH

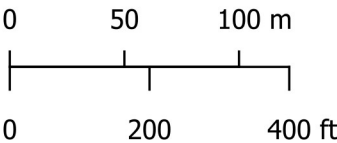
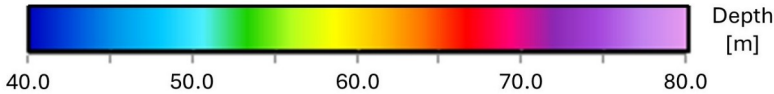


**GEOPHYSICAL
IMAGING
PARTNERS**



Depth of Investigation

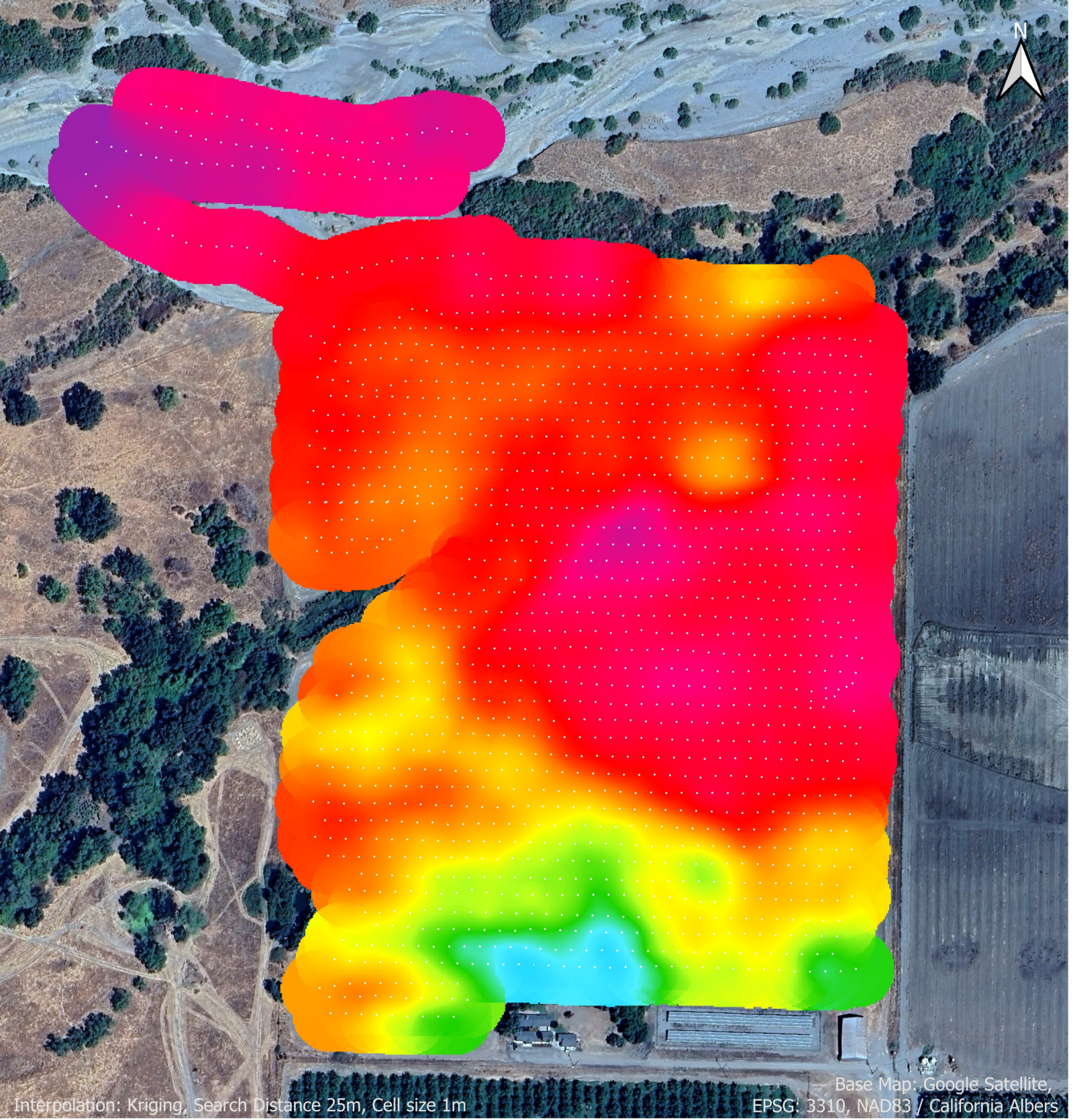
Data Points: Gray dots



Date surveyed: 1/16/2025
Date map created : 03/26/2025
Created by: AAB
Checked by: MH



Appendix 4 – Mean Resistivity Maps

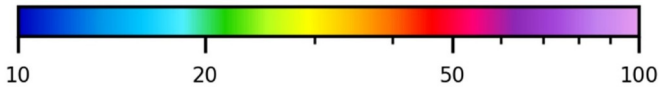
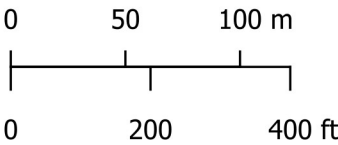


Interpolation: Kriging, Search Distance 25m, Cell size 1m

Base Map: Google Satellite,
EPSG: 3310, NAD83 / California Albers

Mean Resistivity Map
Depth Interval 0-2 meters (0-7 feet)

Data Points: Gray dots

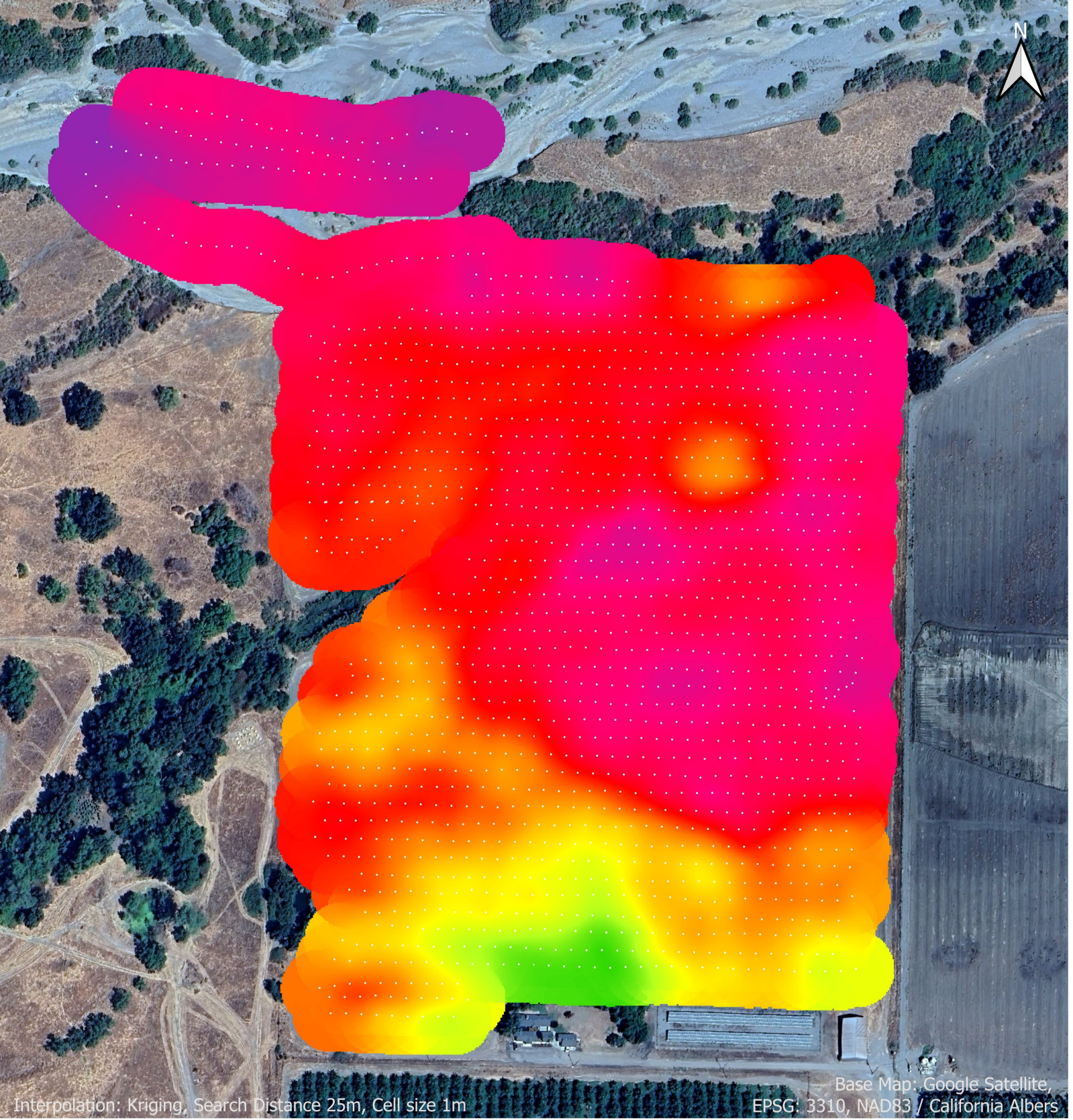


Resistivity
[ohm-m]

Date surveyed: 1/16/2025
Date map created : 03/26/2025
Created by: AAB
Checked by: MH



**GEOPHYSICAL
IMAGING
PARTNERS**

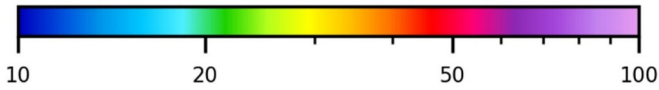
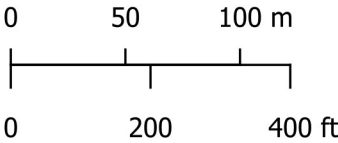


Interpolation: Kriging, Search Distance 25m, Cell size 1m

Base Map: Google Satellite,
EPSG: 3310, NAD83 / California Albers

Mean Resistivity Map
Depth Interval 2-4 meters (7-13 feet)

Data Points: Gray dots

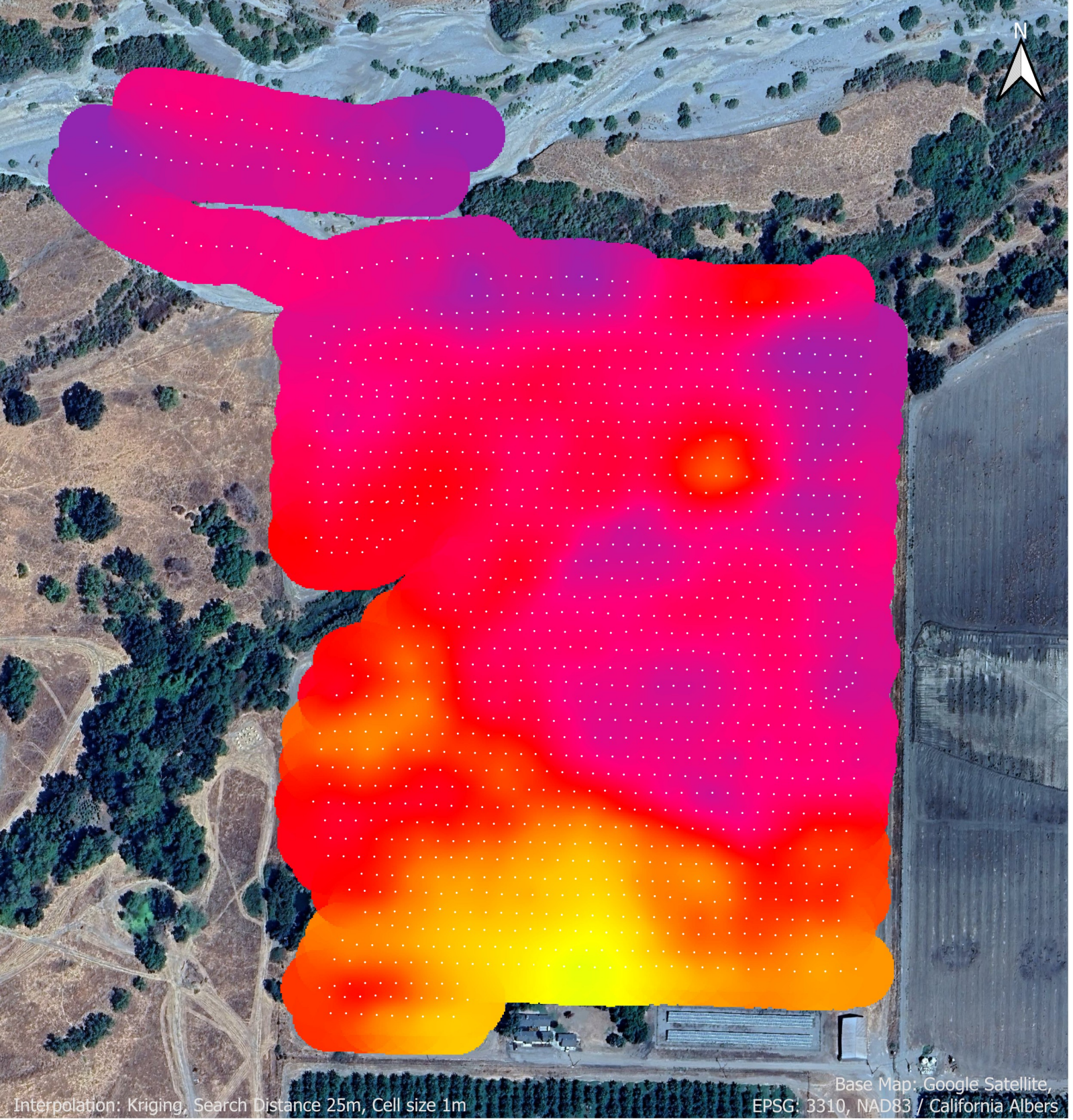


Resistivity
[ohm-m]

Date surveyed: 1/16/2025
Date map created : 03/26/2025
Created by: AAB
Checked by: MH



**GEOPHYSICAL
IMAGING
PARTNERS**

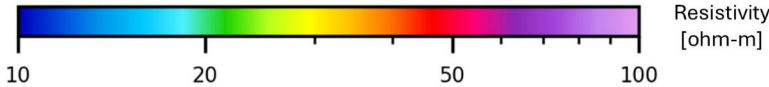
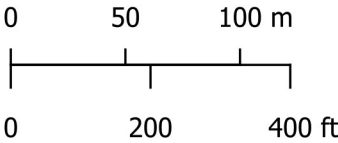


Interpolation: Kriging, Search Distance 25m, Cell size 1m

Base Map: Google Satellite,
EPSG: 3310, NAD83 / California Albers

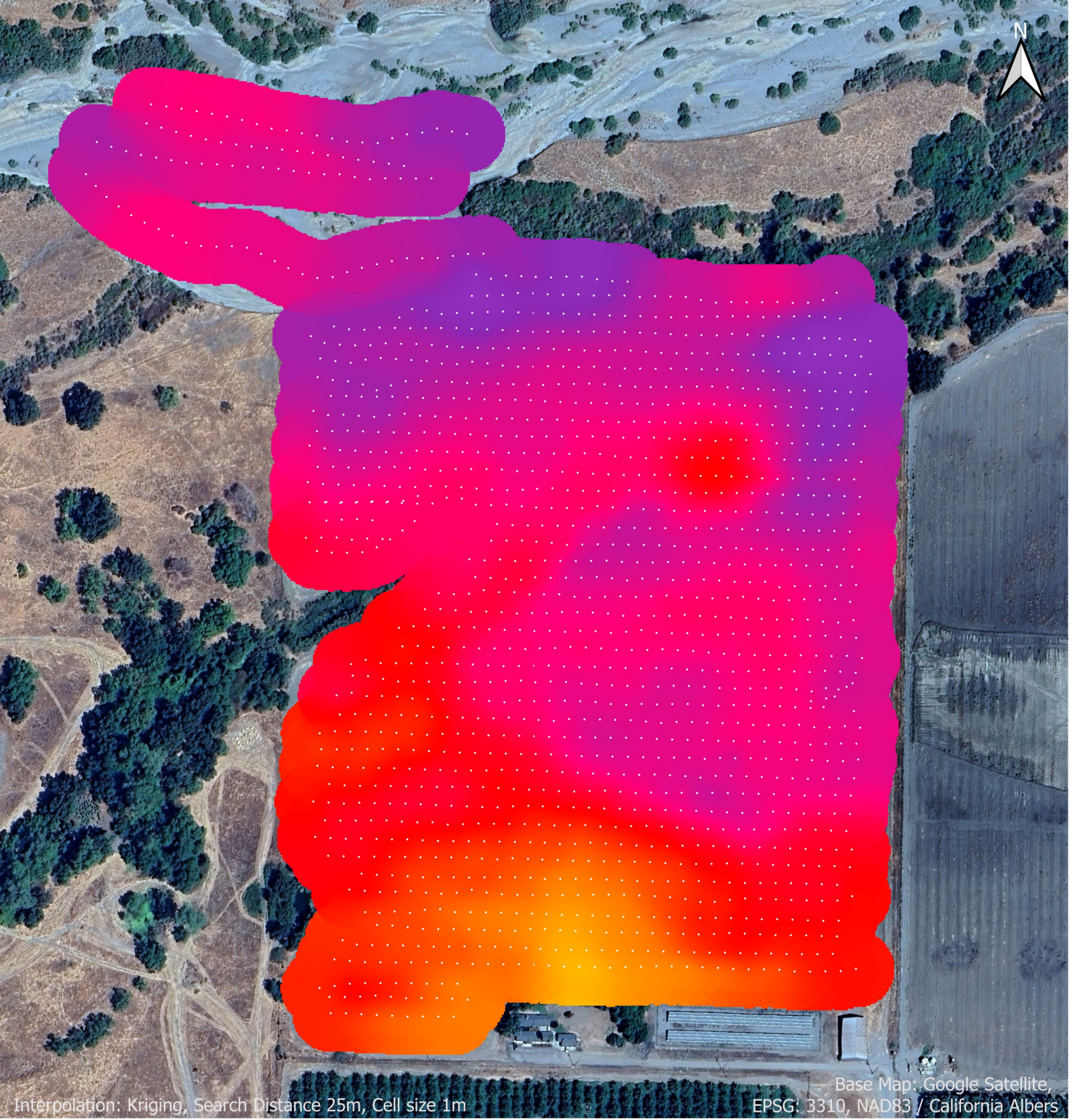
Mean Resistivity Map
Depth Interval 4-6 meters (13-20 feet)

Data Points: Gray dots



Date surveyed: 1/16/2025
Date map created : 03/26/2025
Created by: AAB
Checked by: MH



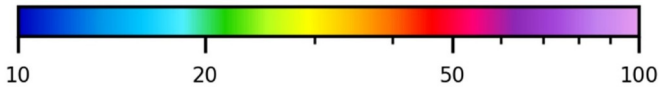
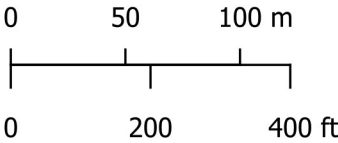


Interpolation: Kriging, Search Distance 25m, Cell size 1m

Base Map: Google Satellite,
EPSG: 3310, NAD83 / California Albers

Mean Resistivity Map
Depth Interval 6-8 meters (20-26 feet)

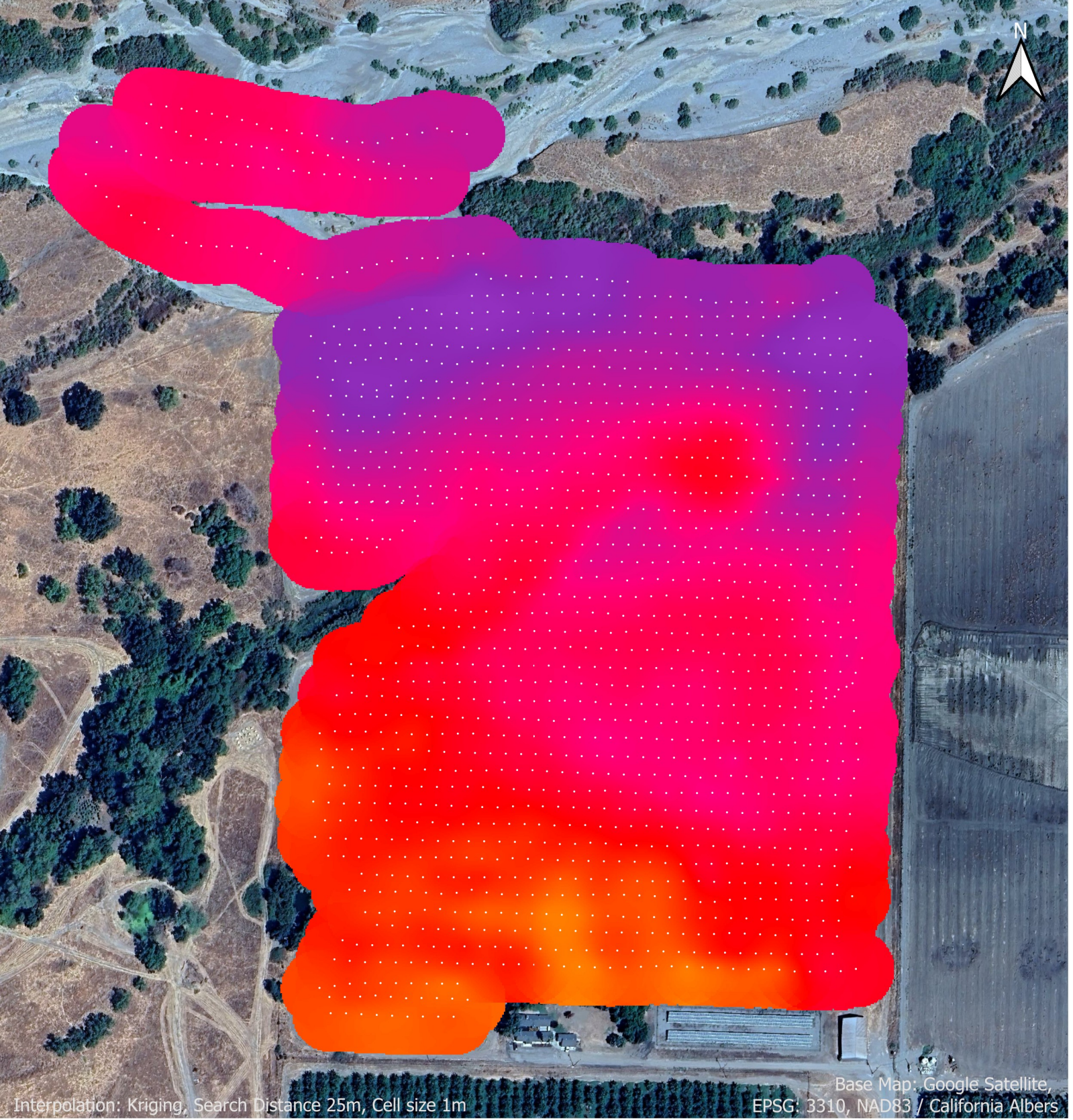
Data Points: Gray dots



Resistivity
[ohm-m]

Date surveyed: 1/16/2025
Date map created : 03/26/2025
Created by: AAB
Checked by: MH



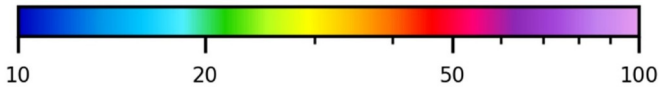
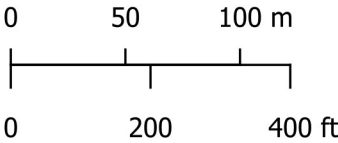


Interpolation: Kriging, Search Distance 25m, Cell size 1m

Base Map: Google Satellite,
EPSG: 3310, NAD83 / California Albers

Mean Resistivity Map
Depth Interval 8-10 meters (26-33 feet)

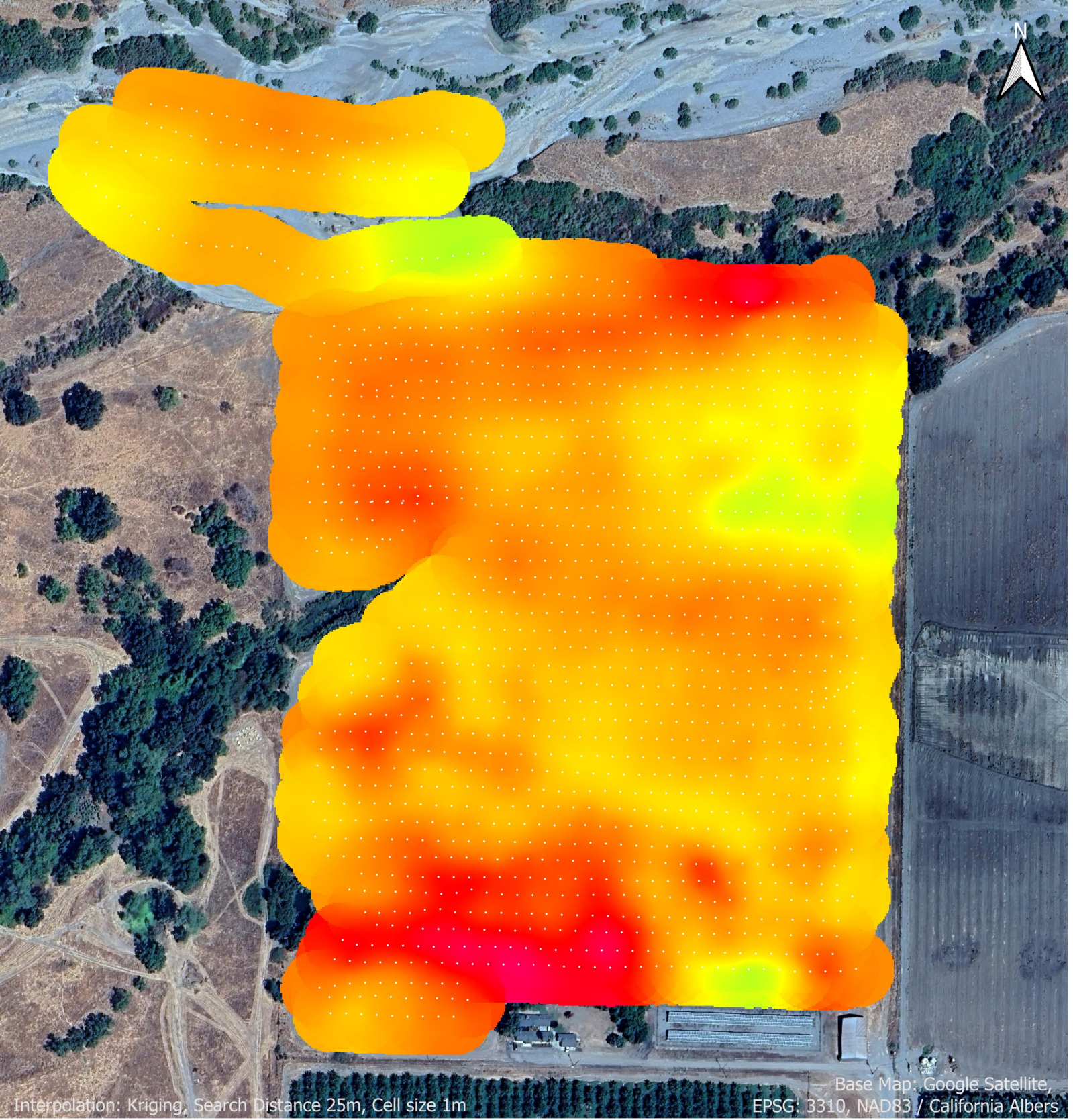
Data Points: Gray dots



Resistivity
[ohm-m]

Date surveyed: 1/16/2025
Date map created : 03/26/2025
Created by: AAB
Checked by: MH



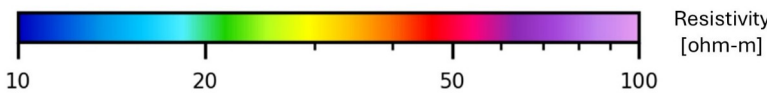
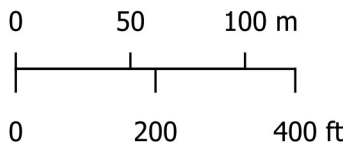


Interpolation: Kriging, Search Distance 25m, Cell size 1m

Base Map: Google Satellite,
EPSG: 3310, NAD83 / California Albers

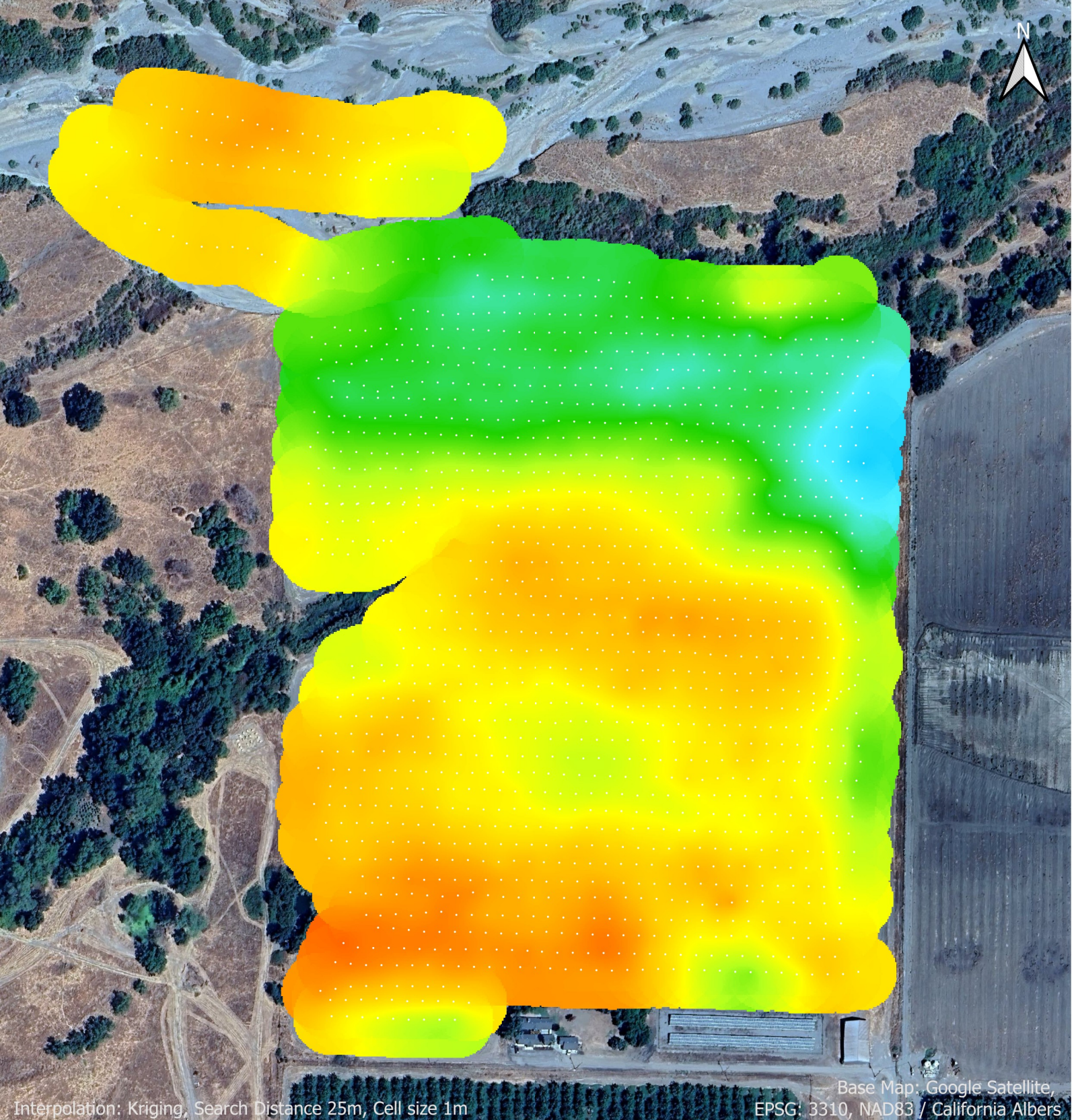
Mean Resistivity Map
Depth Interval 15-20 meters (49-66 feet)

Data Points: Gray dots



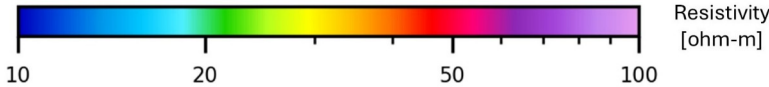
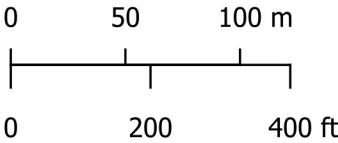
Date surveyed: 1/16/2025
Date map created : 03/26/2025
Created by: AAB
Checked by: MH





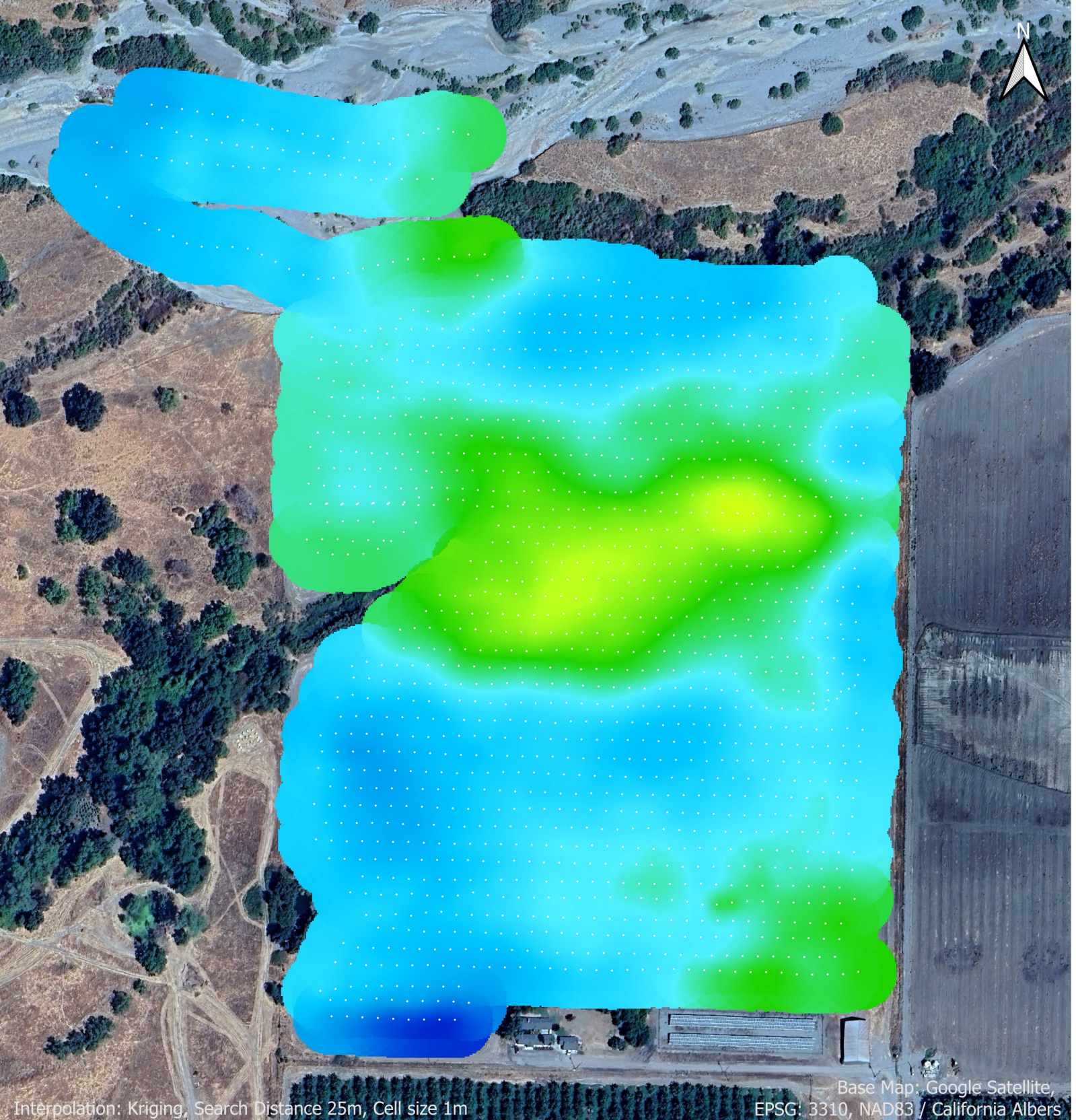
Mean Resistivity Map
Depth Interval 20-30 meters (66-98 feet)

Data Points: Gray dots



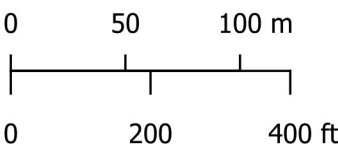
Date surveyed: 1/16/2025
Date map created : 03/26/2025
Created by: AAB
Checked by: MH





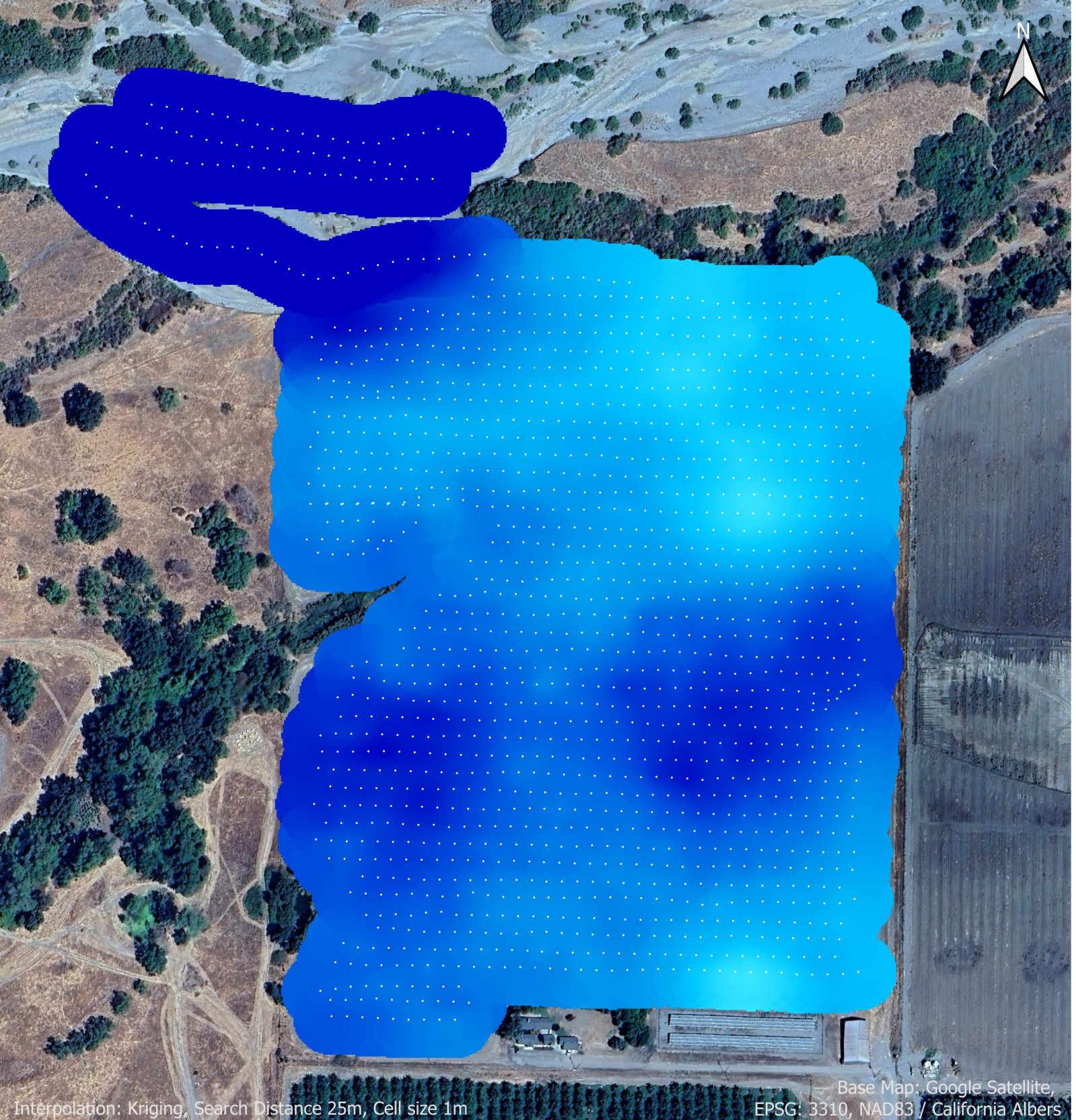
Mean Resistivity Map
Depth Interval 30-40 meters (98-131 feet)

Data Points: Gray dots



Date surveyed: 1/16/2025
Date map created : 03/26/2025
Created by: AAB
Checked by: MH



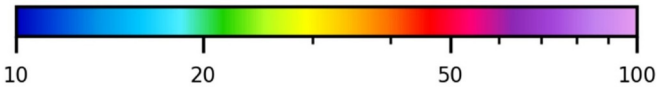
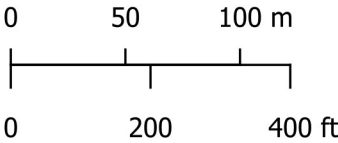


Interpolation: Kriging, Search Distance 25m, Cell size 1m

Base Map: Google Satellite,
EPSG: 3310, NAD83 / California Albers

Mean Resistivity Map
Depth Interval 40-50 meters (131-164 feet)

Data Points: Gray dots

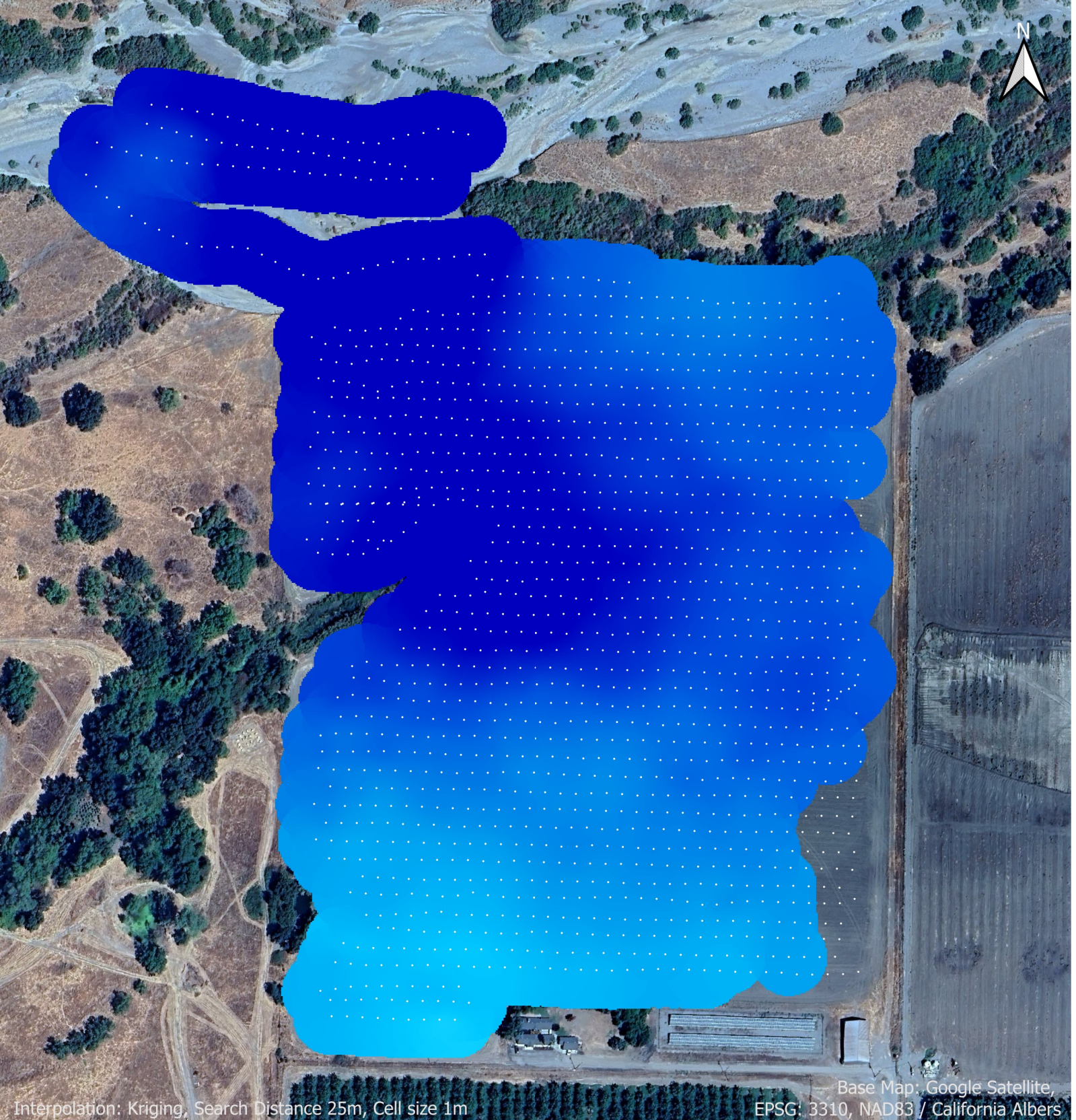


Resistivity
[ohm-m]

Date surveyed: 1/16/2025
Date map created : 03/26/2025
Created by: AAB
Checked by: MH



**GEOPHYSICAL
IMAGING
PARTNERS**

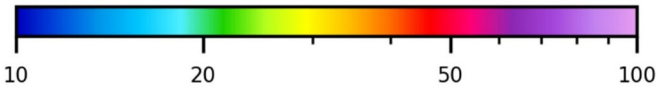
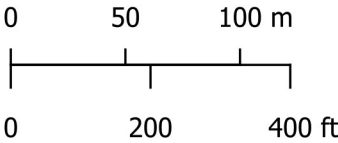


Interpolation: Kriging, Search Distance 25m, Cell size 1m

Base Map: Google Satellite,
EPSG: 3310, NAD83 / California Albers

Mean Resistivity Map
Depth Interval 50-60 meters (164-197 feet)

Data Points: Gray dots

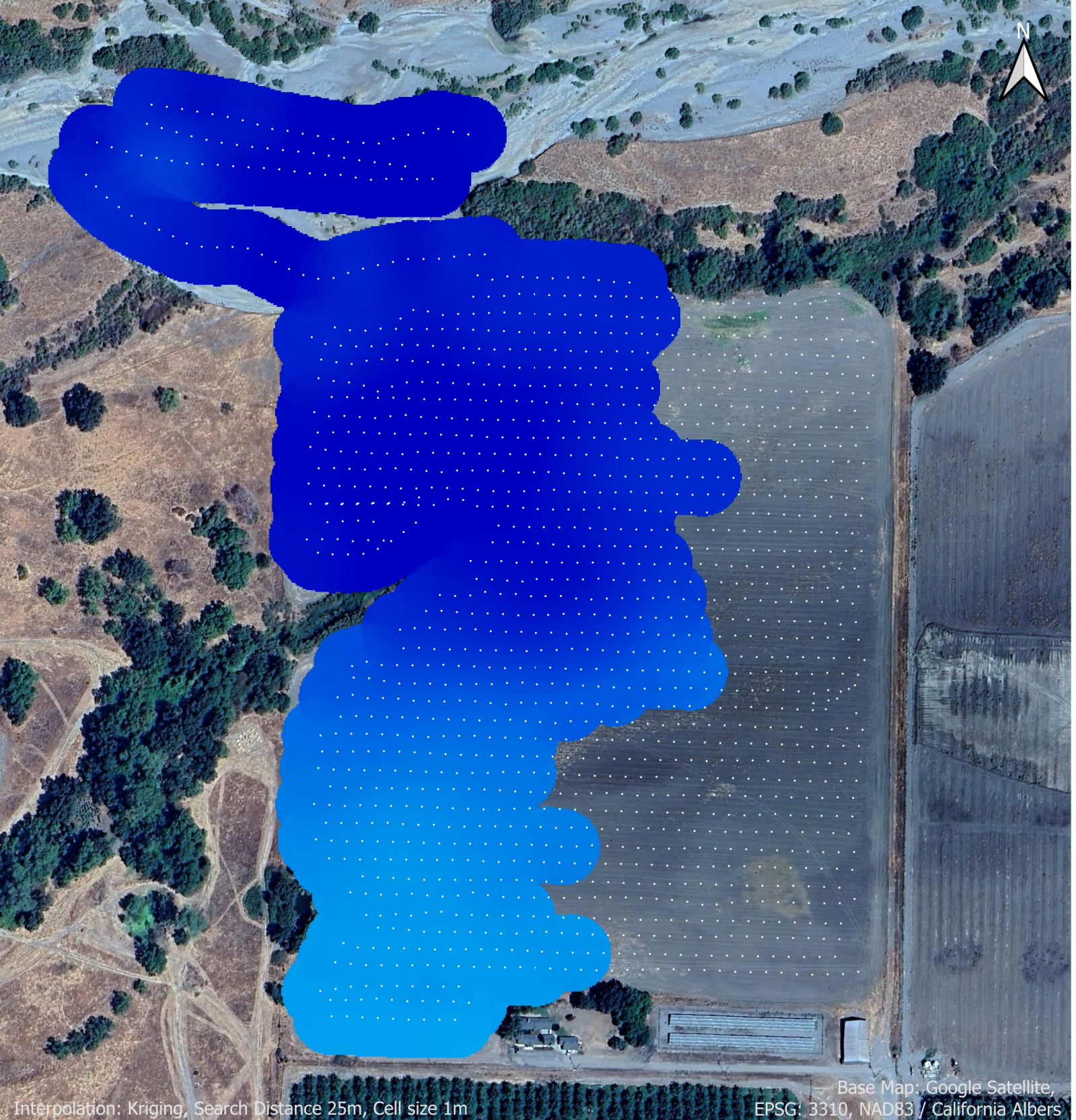


Resistivity
[ohm-m]

Date surveyed: 1/16/2025
Date map created : 03/26/2025
Created by: AAB
Checked by: MH



**GEOPHYSICAL
IMAGING
PARTNERS**

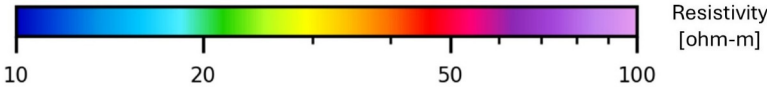
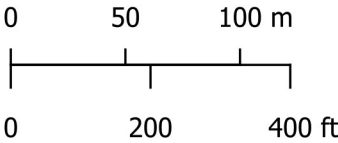


Interpolation: Kriging, Search Distance 25m, Cell size 1m

Base Map: Google Satellite,
EPSG: 3310, NAD83 / California Albers

Mean Resistivity Map
Depth Interval 60-80 meters (197-262 feet)

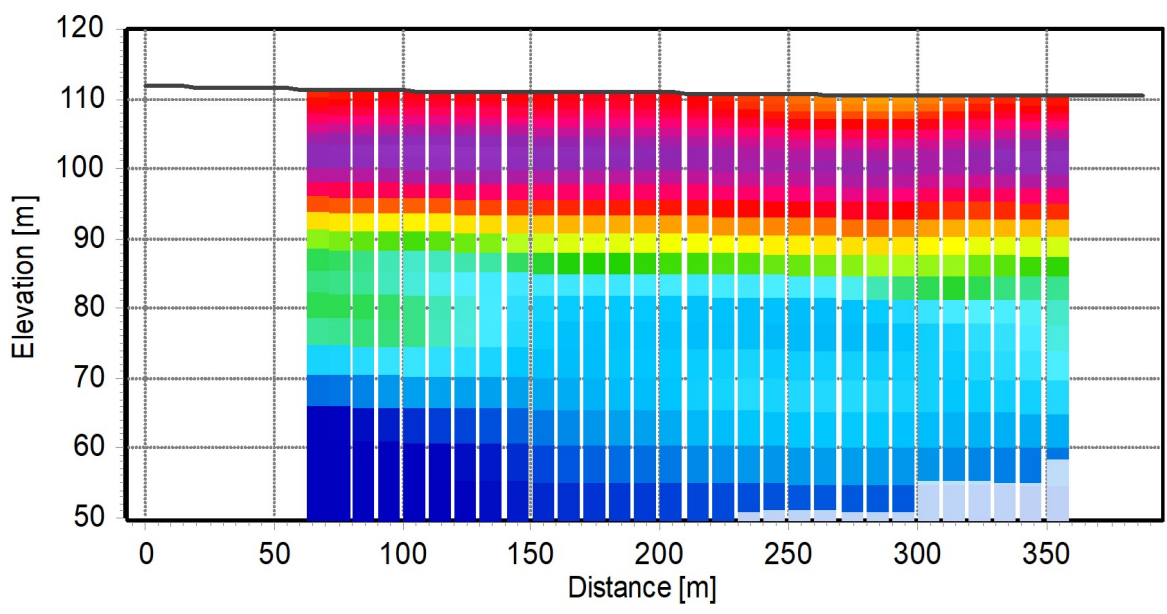
Data Points: Gray dots



Date surveyed: 1/16/2025
Date map created : 03/26/2025
Created by: AAB
Checked by: MH

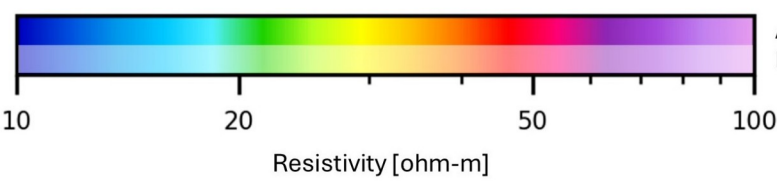
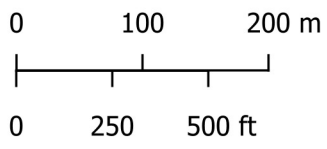


Appendix 5 – Vertical Sections



Vertical Section P01 W-E

— Location of Vertical Section

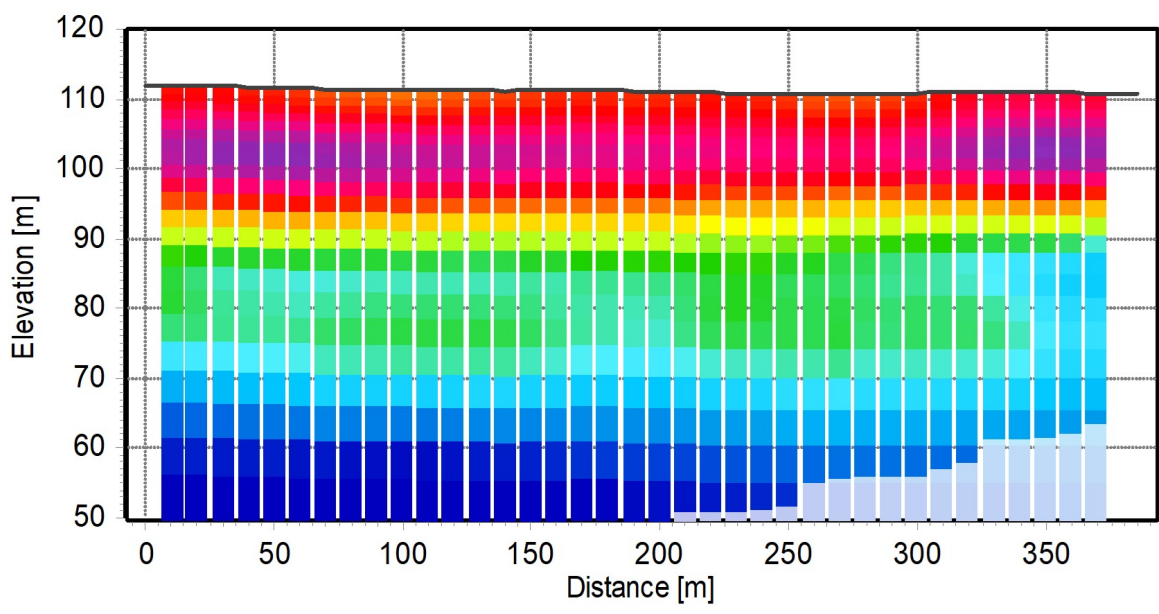


Above DOI
Below DOI

*) Depth of investigation

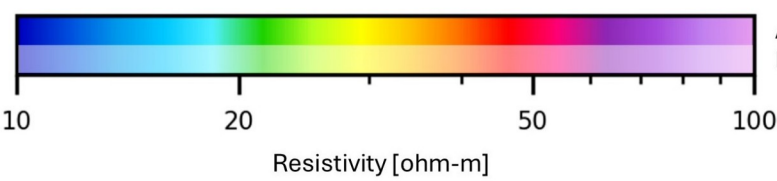
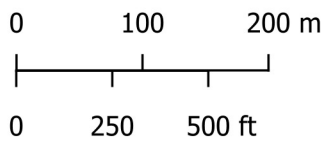
Project: 24003
Date surveyed: 1/16/2025
Date map created: 03/27/2025
Created by: AAB
Checked by: MH





Vertical Section P02 W-E

— Location of Vertical Section

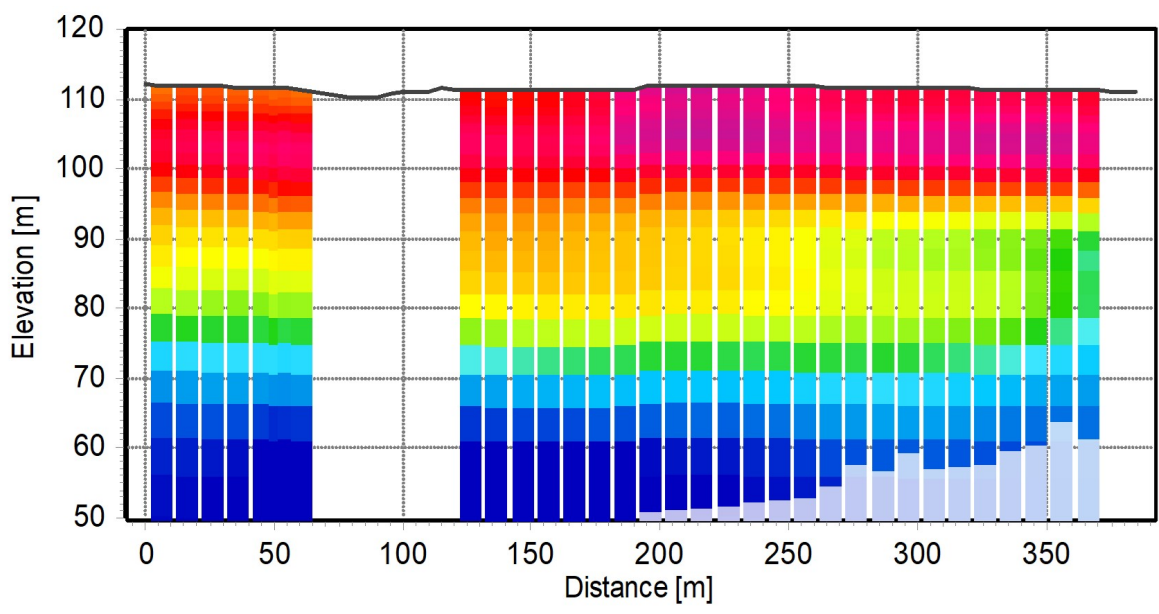
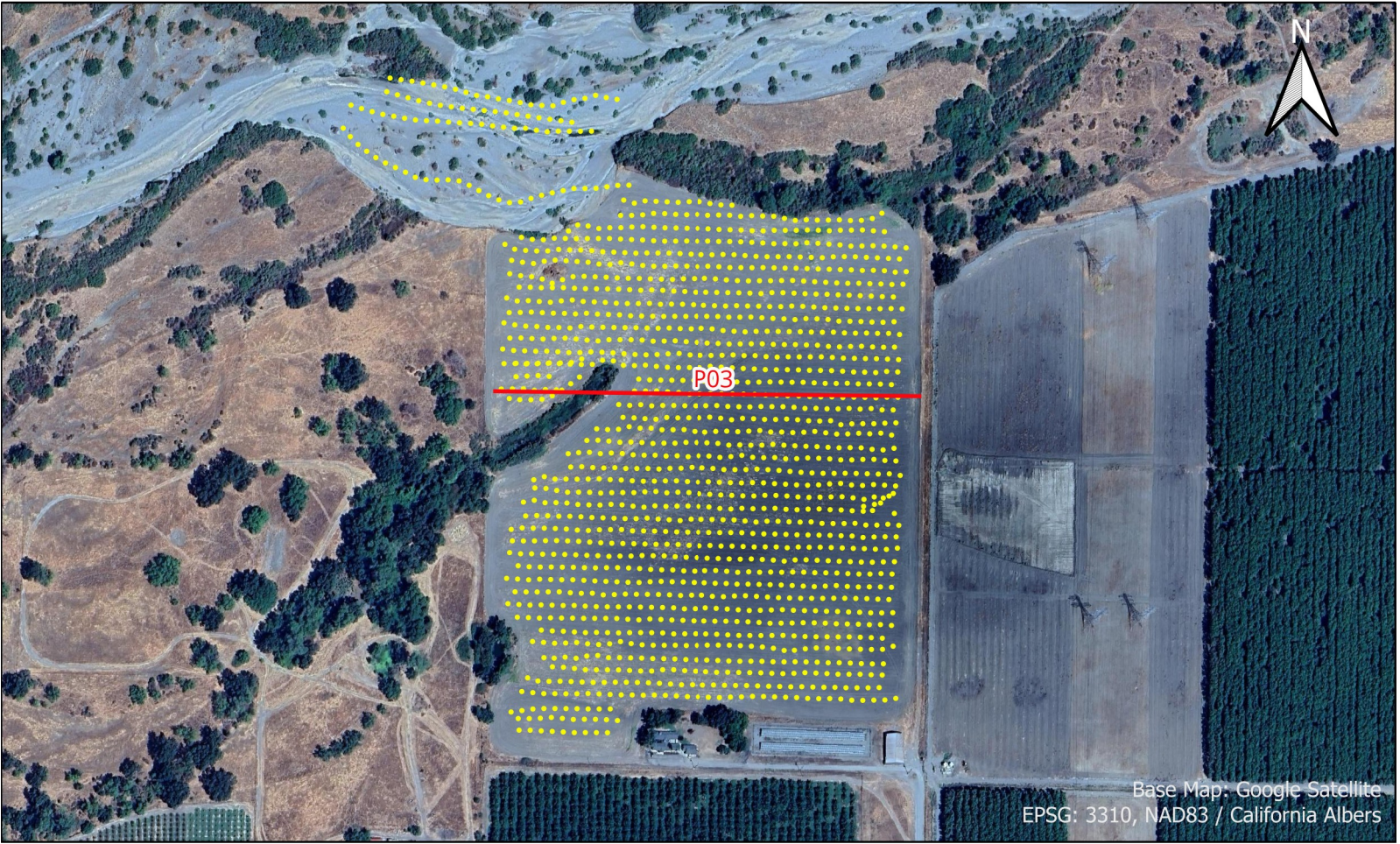


Above DOI
Below DOI

*) Depth of investigation

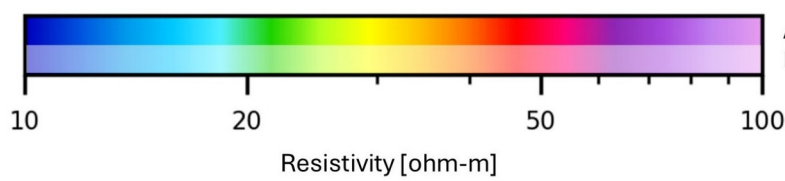
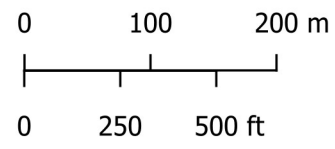
Project: 24003
Date surveyed: 1/16/2025
Date map created: 03/27/2025
Created by: AAB
Checked by: MH





Vertical Section P03 W-E

— Location of Vertical Section

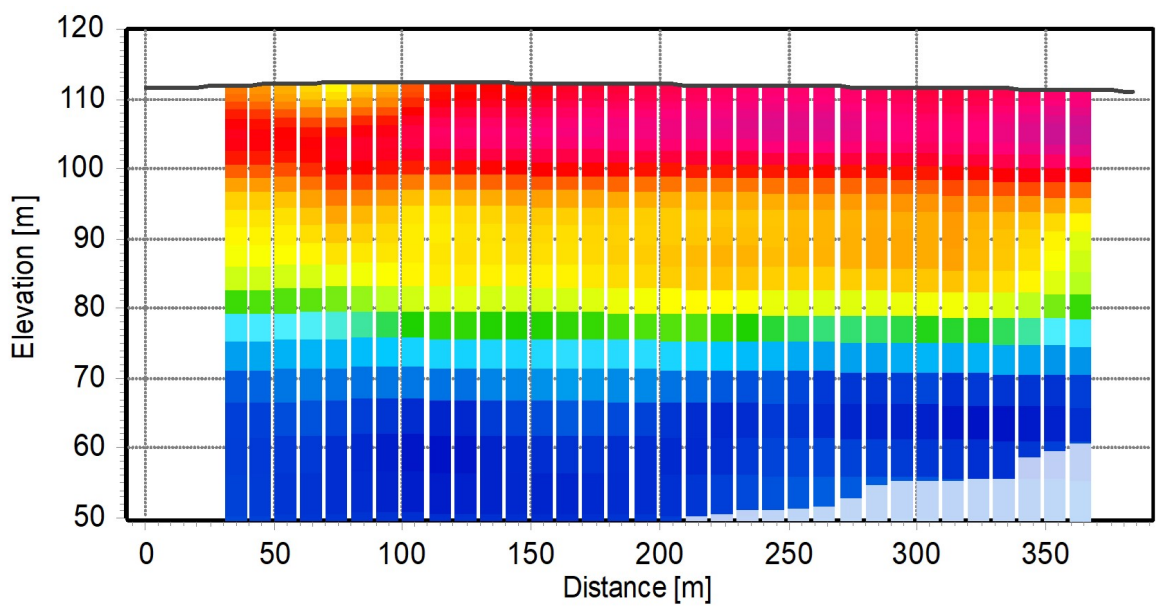


Above DOI
Below DOI

*) Depth of investigation

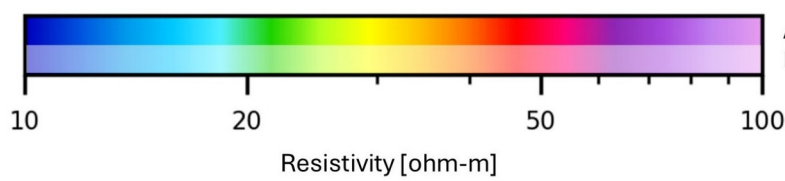
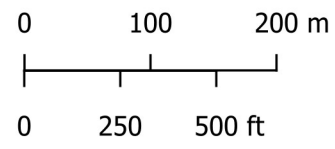
Project: 24003
Date surveyed: 1/16/2025
Date map created: 03/27/2025
Created by: AAB
Checked by: MH





Vertical Section P04 W-E

— Location of Vertical Section

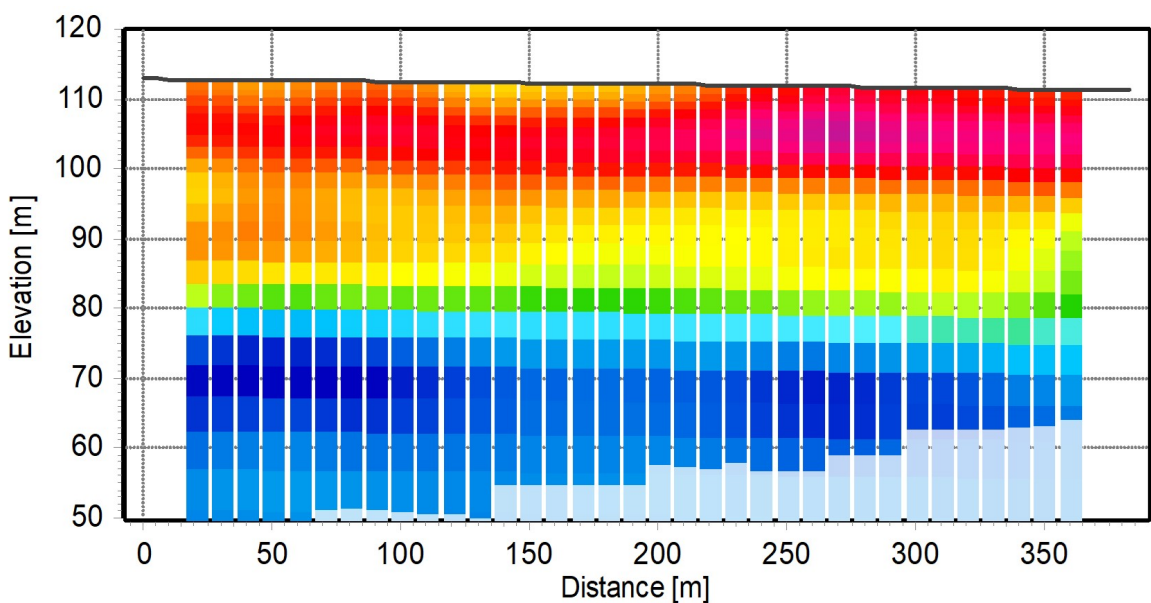


Above DOI*
Below DOI

*) Depth of investigation

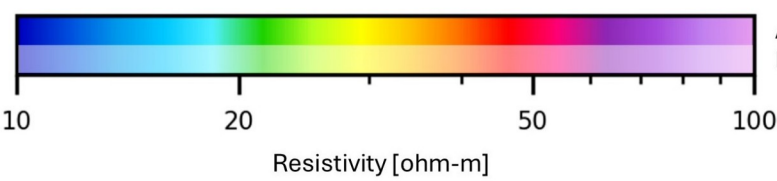
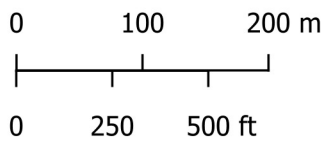
Project: 24003
Date surveyed: 1/16/2025
Date map created: 03/27/2025
Created by: AAB
Checked by: MH





Vertical Section P05 W-E

— Location of Vertical Section

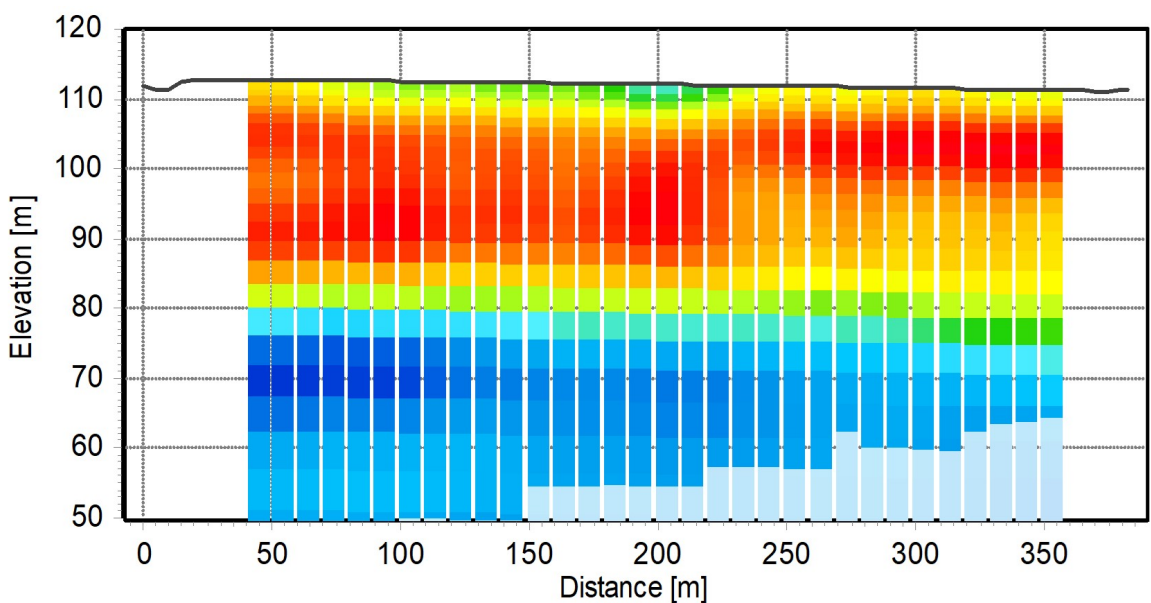
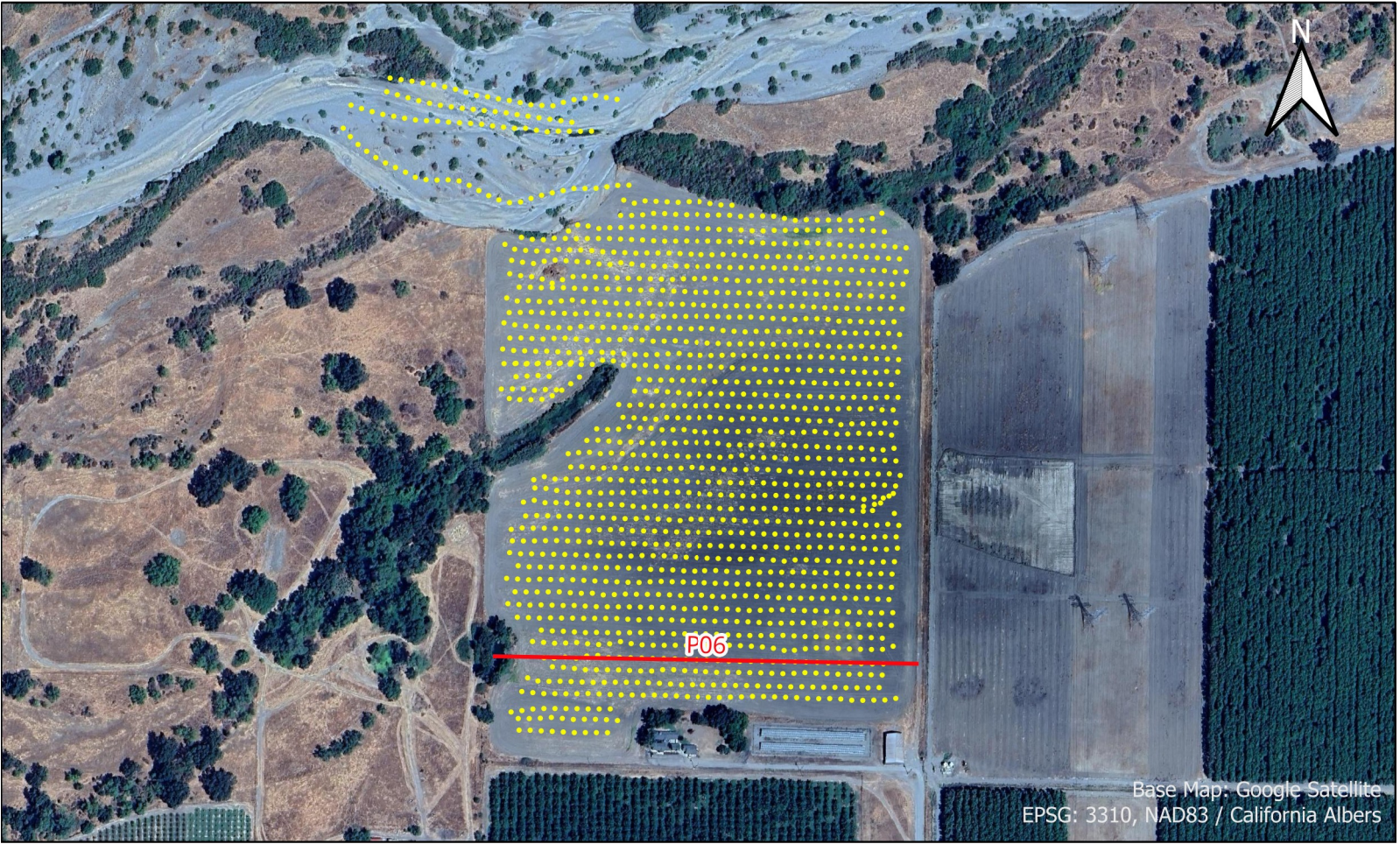


Above DOI
Below DOI

*) Depth of investigation

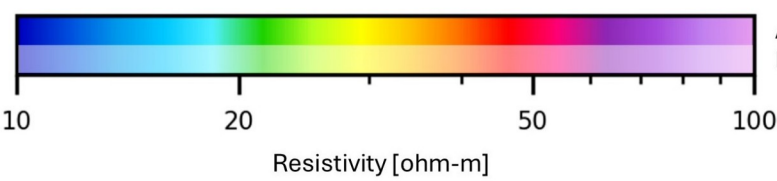
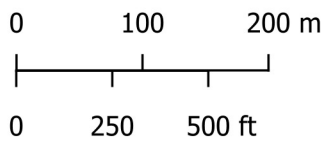
Project: 24003
Date surveyed: 1/16/2025
Date map created: 03/27/2025
Created by: AAB
Checked by: MH





Vertical Section P06 W-E

— Location of Vertical Section

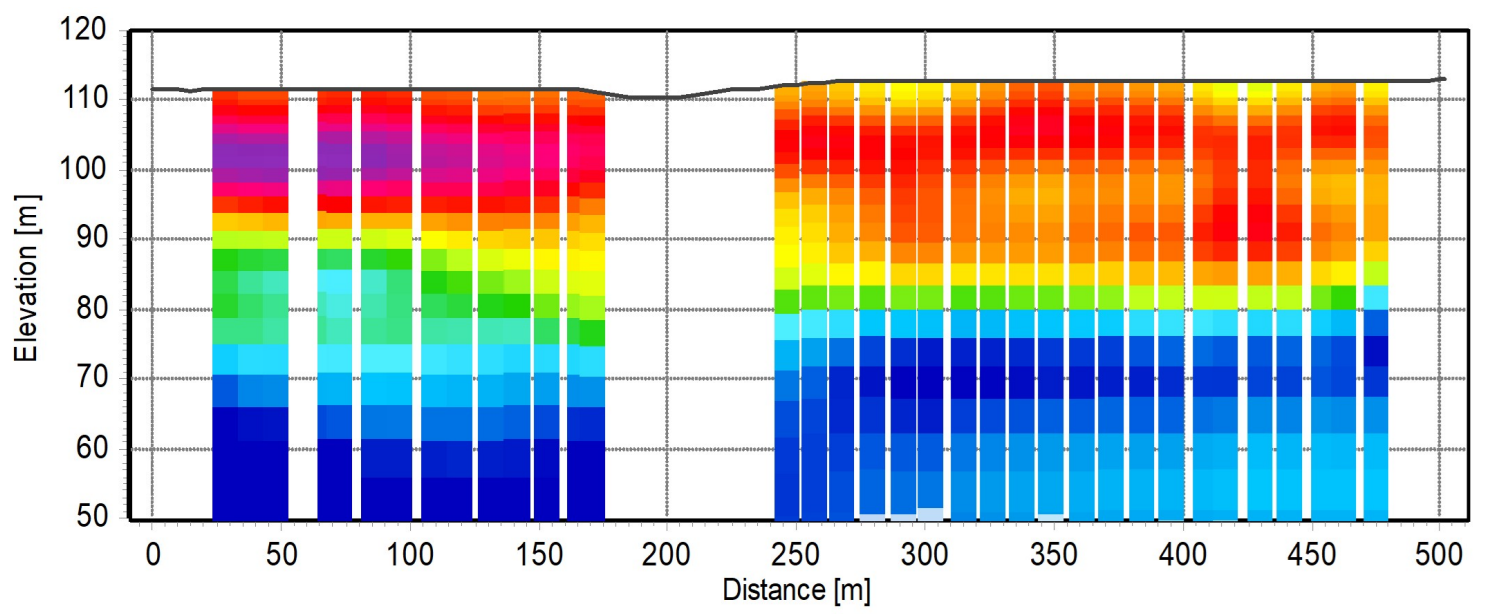


Above DOI
Below DOI

*) Depth of investigation

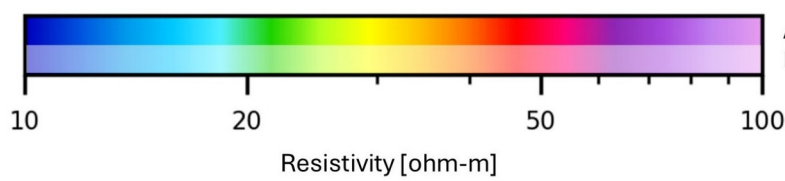
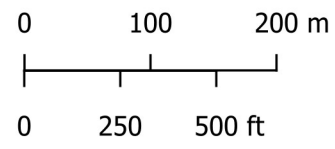
Project: 24003
Date surveyed: 1/16/2025
Date map created: 03/27/2025
Created by: AAB
Checked by: MH





Vertical Section P07 N-S

— Location of Vertical Section

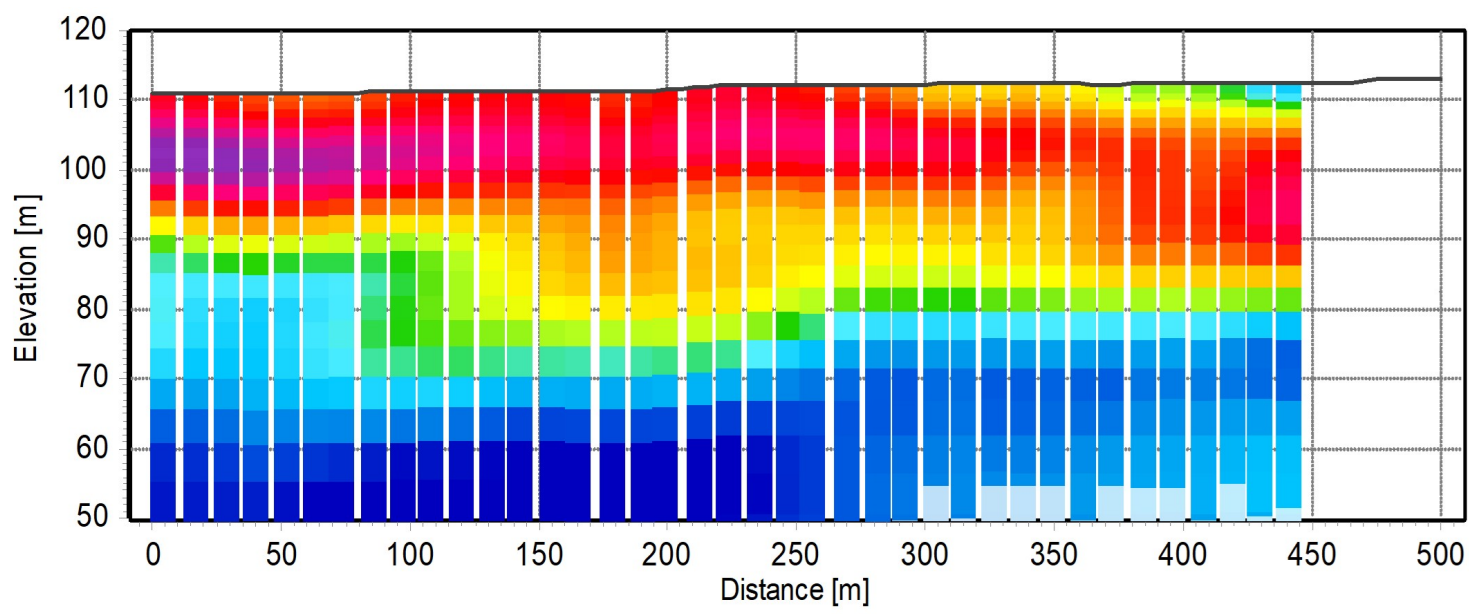


Above DOI
Below DOI

*) Depth of investigation

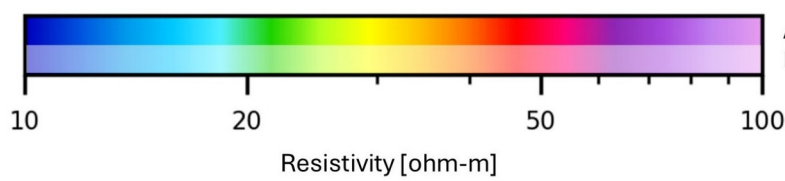
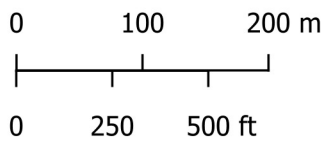
Project: 24003
Date surveyed: 1/16/2025
Date map created: 03/27/2025
Created by: AAB
Checked by: MH





Vertical Section P08 N-S

— Location of Vertical Section

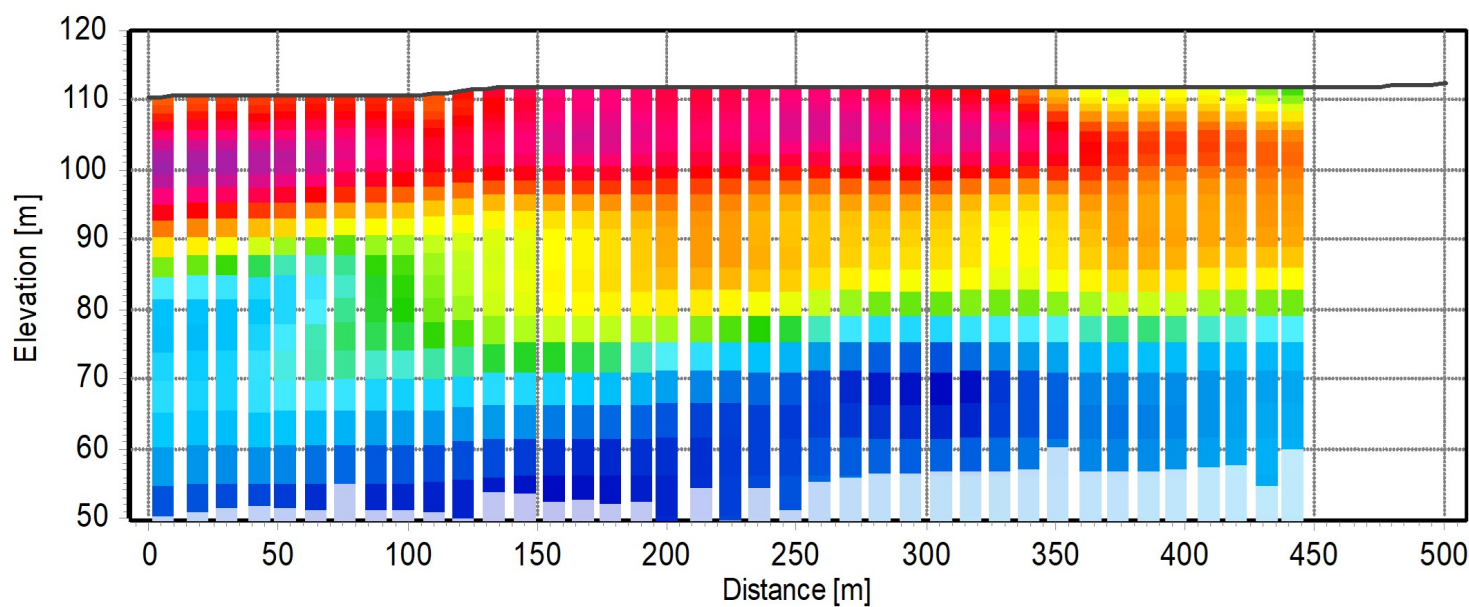


Above DOI
Below DOI

*) Depth of investigation

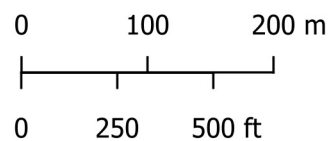
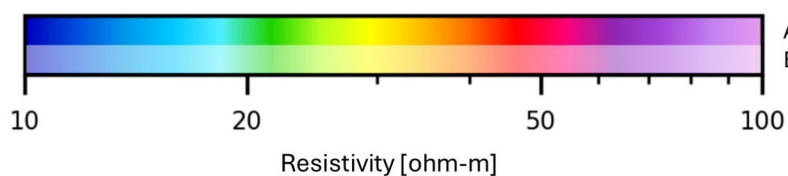
Project: 24003
Date surveyed: 1/16/2025
Date map created: 03/27/2025
Created by: AAB
Checked by: MH





Vertical Section P09 N-S

— Location of Vertical Section

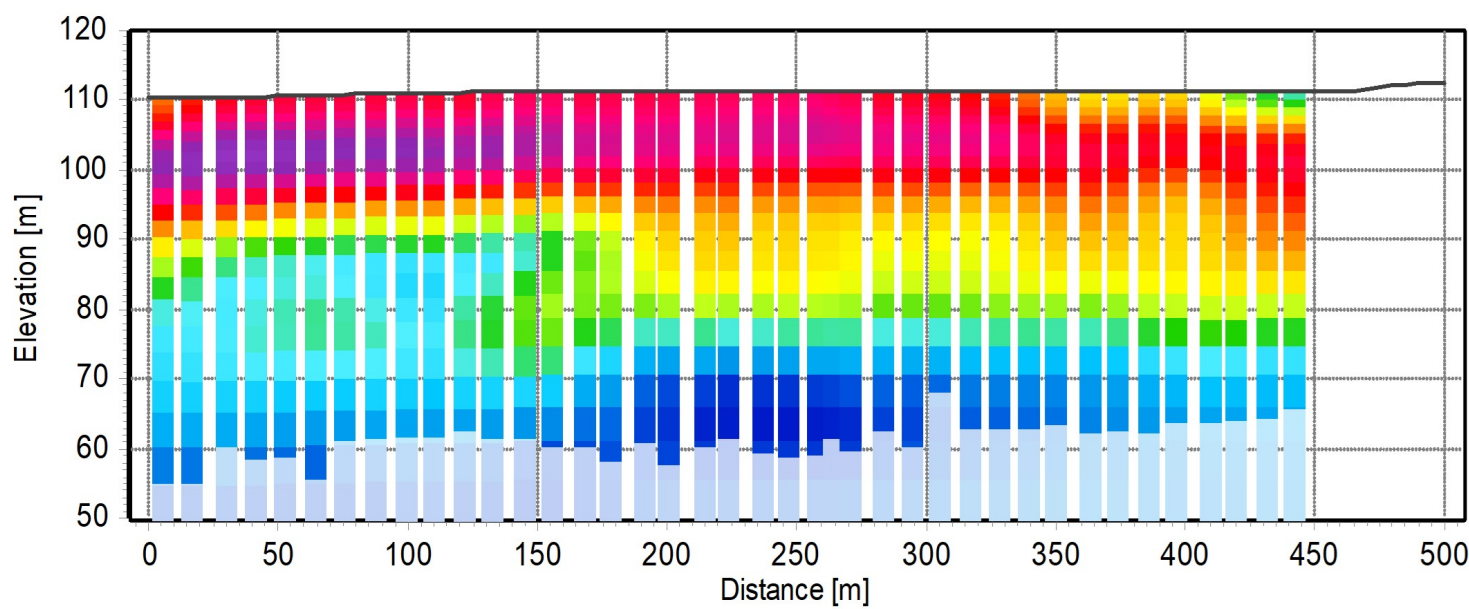


Above DOI
Below DOI

*) Depth of investigation

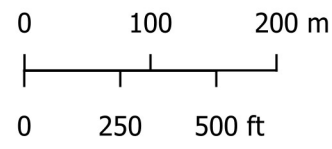
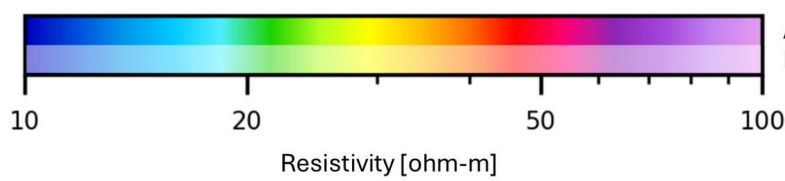
Project: 24003
Date surveyed: 1/16/2025
Date map created: 03/27/2025
Created by: AAB
Checked by: MH





Vertical Section P10 N-S

— Location of Vertical Section

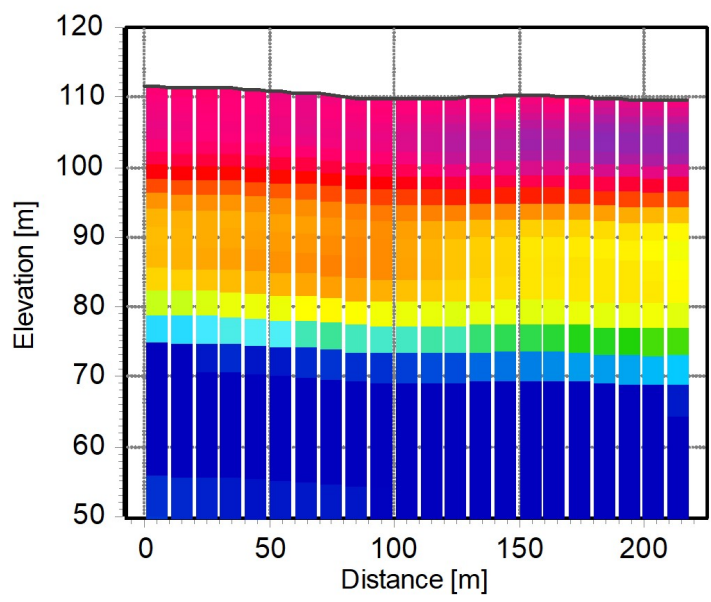


Above DOI
Below DOI

*) Depth of investigation

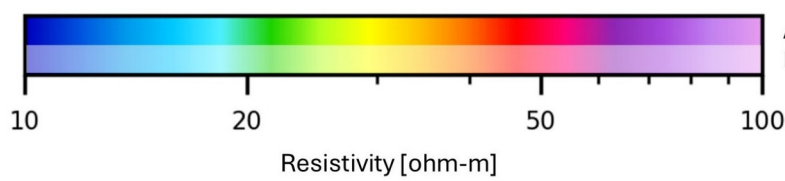
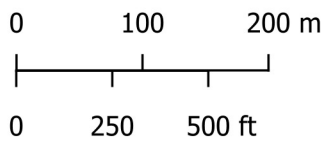
Project: 24003
Date surveyed: 1/16/2025
Date map created: 03/27/2025
Created by: AAB
Checked by: MH





Vertical Section P11 W-E

— Location of Vertical Section

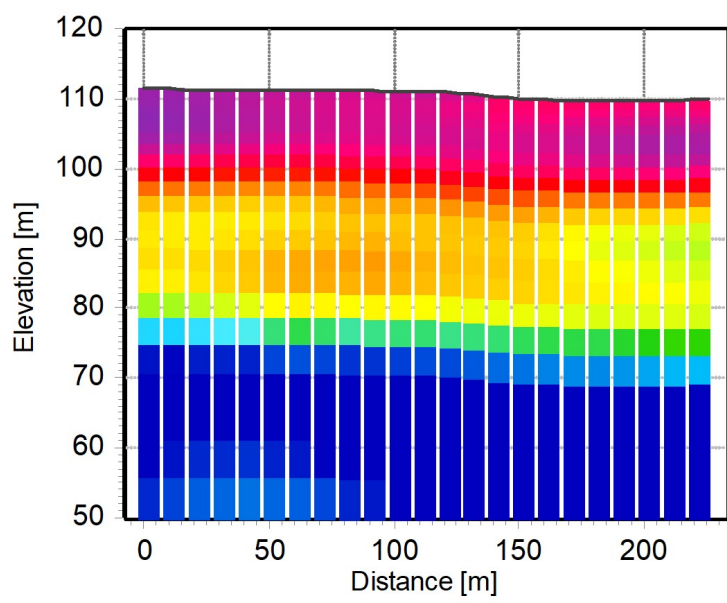
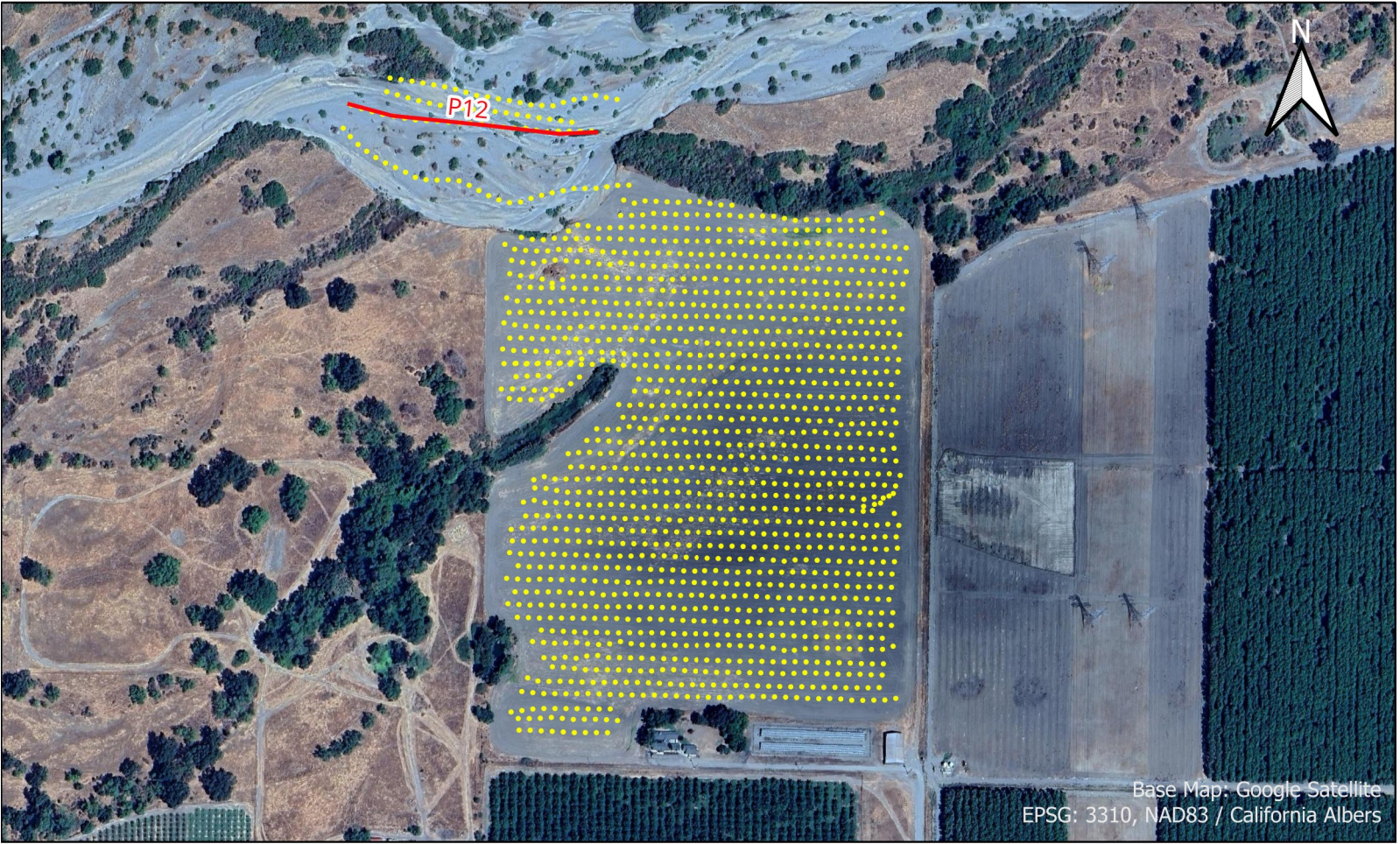


Above DOI
Below DOI

*) Depth of investigation

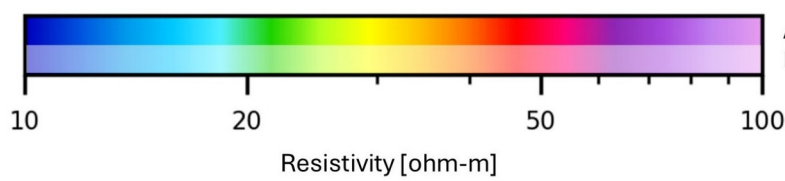
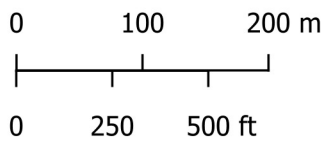
Project: 24003
Date surveyed: 1/16/2025
Date map created: 03/27/2025
Created by: AAB
Checked by: MH





Vertical Section P12 W-E

— Location of Vertical Section

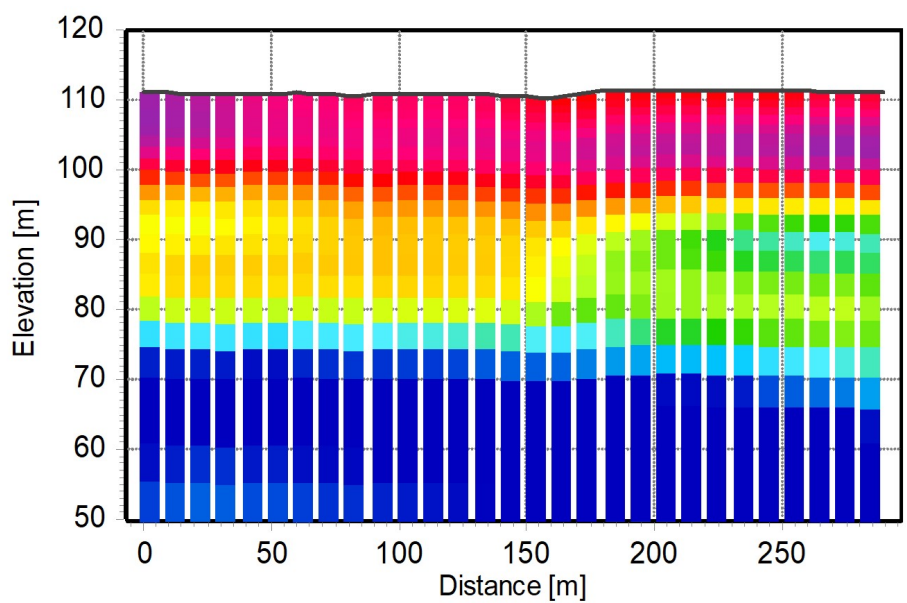
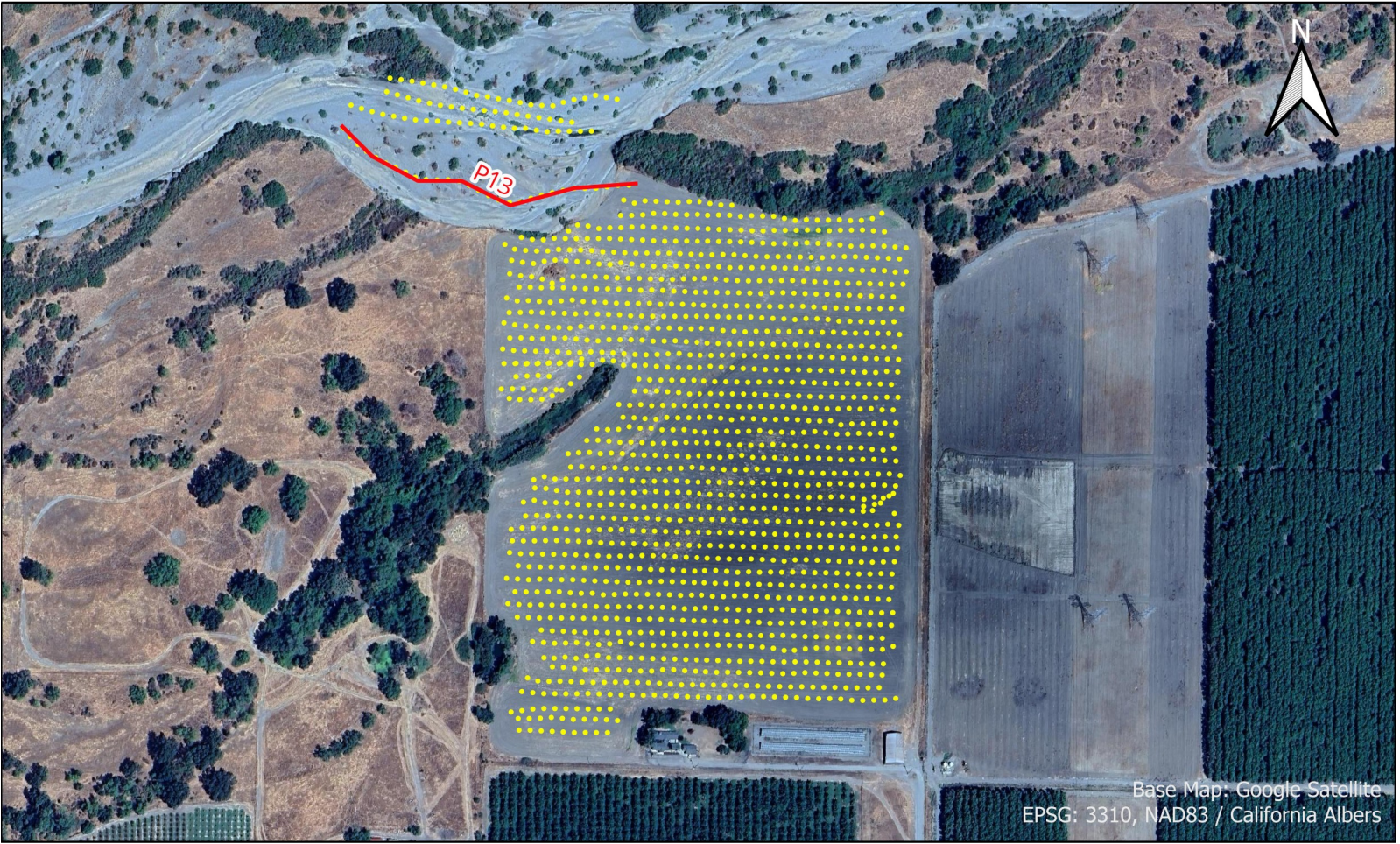


Above DOI
Below DOI

*) Depth of investigation

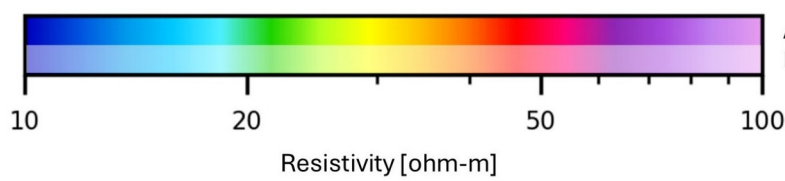
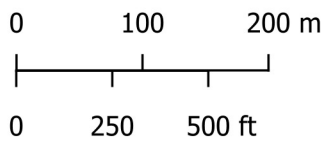
Project: 24003
Date surveyed: 1/16/2025
Date map created: 03/27/2025
Created by: AAB
Checked by: MH





Vertical Section P13 W-E

— Location of Vertical Section



Above DOI
Below DOI
*) Depth of investigation

Project: 24003
Date surveyed: 1/16/2025
Date map created: 03/27/2025
Created by: AAB
Checked by: MH



Appendix 6 – A description of the digital data formats

For each model type (multi-layer model/smooth model or few-layer model/sharp model), data can be exported in different formats to facilitate import and management of data in third-party software solutions. Below are descriptions of four ASCII formats (*_byLayer.xyz, *_syn.xyz, *_inv.xyz, *_dat.xyz). The file named *Project_byLayer.xyz* might be the most generic format, suitable for visualization in software packages like Leapfrog, Rockworks, EVS, and similar. In addition to the four ASCII files, georeferenced raster files (Geotiffs) and ArcGIS shape files are provided as part of the data deliverables.

The *_byLayer.xyz file uses the following format:

Header section:

```
/INFO

/Aarhus SPIA export file. File created: 30-03-2023 13:00:34. Exported from SPIA64

/SPIA VERSION          3.7.0.0

/PROJECT NAME          Projectname.gdb

/DUMMY

/9999

/DATATYPE              Type of data

/COORDINATE SYSTEM     Coordinate System: WGS 84 UTM zone 19S (epsg:32719)

/NUMBER OF LAYERS      6 Max Number of layers

/MODEL UNIT             Base unit used for resistivities: /Resistivity (Ohm-m) / conductivity
(mS/m)

/LENGTH UNIT          Base unit used for distances: Meter
```

Main section:

```
ID                      Incrementing number

LINE_NO                Line number

LAYER_NO               Layer number

UTMX                   UTMX

UTMY                   UTMY

ELEVATION_CELL         Elevation top of Layer

RESISTIVITY            Resistivity

RESISTIVITY_STD        STD on Resistivity

CONDUCTIVITY           Conductivity

DEPTH_TOP              Depth to top of layer

DEPTH_BOTTOM           Depth to bottom of layer

THICKNESS              Thickness of layer

THICKNESS_STD          STD on Layer Thickness
```


The *_SYN.xyz file use the following format:

Header section:

```
/INFO
/Aarhus SPIA export file. File created: 30-03-2023 13:00:34. Exported from SPIA64
/SPIA VERSION          3.7.0.0
/PROJECT NAME          ProjectName.gdb
/DUMMY
/9999
/DATATYPE              Type of data
/COORDINATE SYSTEM     Coordinate System: WGS 84 UTM zone 19S (epsg:32719)
/NUMBER OF LAYERS      30 Number of layers
/MODEL UNIT            Base unit used for resistivities: /Resistivity (Ohm-m) / conductivity
(mS/m)
/LENGTH UNIT          Base unit used for distances: Meter
```

Main section:

```
LINE_NO              Line number
MODEL_NAME           Model Name
UTMX                 UTMX
UTMY                 UTMY
DATE                 Dummy value
TIME                 Dummy value
RECORD               Record
ELEVATION            Topography
NUMDATA              Number of gates inverted
SEGMENT              Moment ID (low moment=1, high moment=2)
RESDATA              Data misfit (normalized with STD)
RESTOTAL             Total misfit
DATA_1               Voltage (V/Am^4), for gate_1
DATA_2               Voltage (V/Am^4), for gate_2
...
DATA_N               Voltage (V/Am^4), for gate_N
```

The *_inv.xyz file use the following format:

Header section:

```
/INFO

/Aarhus SPIA export file. File created: 30-03-2023 13:00:34. Exported from SPIA64

/SPIA VERSION          3.7.0.0

/PROJECT NAME          ProjectName.gdb

/DUMMY

/9999

/DATATYPE              Type of data

/COORDINATE SYSTEM     Coordinate System: WGS 84 UTM zone 19S (epsg:32719)

/NUMBER OF LAYERS      30 Number of layers

/MODEL UNIT            Base unit used for resistivities: /Resistivity (Ohm-m) / conductivity
(mS/m)

/LENGTH UNIT          Base unit used for distances: Meter
```

Main section:

```
LINE_NO              Line number (always 0)

UTMX                 UTMX

UTMY                 UTMY

DATE                 Dummy value

TIME                 Dummy value

RECORD               Record

ELEVATION             Topography

NUMDATA              Number of gates inverted

SEGMENT              Moment ID (low moment=1, high moment=2)

RESDATA              Data misfit (normalized with STD)

RESTOTAL             Total misfit

RHO_I_1              Resistivity (Ohm m) for layer_1

RHO_I_2              Resistivity (Ohm m) for layer_2

...

RHO_I_N              Resistivity (Ohm m) for layer_N

RHO_I_STD_1          STD on resistivity for layer_1

RHO_I_STD_2          STD on resistivity for layer_2

...

RHO_I_STD_N          STD on resistivity for layer_N
```


SIGMA_I_1	Conductivity (mS/m) for layer_1
SIGMA_I_2	Conductivity (mS/m) for layer_2
...	...
SIGMA_I_N	Conductivity (mS/m) for layer_N
IP_P1_I_1	IP parameter 1 for layer_1
IP_P1_I_2	IP parameter 1 for layer_2
...	...
IP_P1_I_N	IP parameter 1 for layer_N
IP_P1_I_STD_1	STD on IP parameter 1 for layer_1
IP_P1_I_STD_2	STD on IP parameter 1 for layer_2
...	...
IP_P1_I_STD_N	STD on IP parameter 1 for layer_N
IP_P2_I_1	IP parameter 2 for layer_1
IP_P2_I_2	IP parameter 2 for layer_2
...	...
IP_P2_I_N	IP parameter 2 for layer_N
IP_P2_I_STD_1	STD on IP parameter 2 for layer_1
IP_P2_I_STD_2	STD on IP parameter 2 for layer_2
...	...
IP_P2_I_STD_N	STD on IP parameter 2 for layer_N
...	...
IP_PM_I_1	IP parameter M for layer_1
IP_PM_I_2	IP parameter M for layer_2
...	...
IP_PM_I_N	IP parameter M for layer_N
IP_PM_I_STD_1	STD on IP parameter M for layer_1
IP_PM_I_STD_2	STD on IP parameter M for layer_2
...	...
IP_PM_I_STD_N	STD on IP parameter M for layer_N
DEP_TOP_1	Depth (m) to top of layer_1
DEP_TOP_2	Depth (m) to top of layer_2
...	...
DEP_TOP_N	Depth (m) to top of layer_N
DEP_BOT_1	Depth (m) to botttom of layer_1
DEP_BOT_2	Depth (m) to botttom of layer_2

...	...
DEP_BOT_N-1	Depth (m) to botttom of layer_N-1
DEP_BOT_N	Depth (m) to bottom of layer_N calculated as 1.5 times DEP_BOT_N-1
THK_1	Thickness (m) of layer_1
THK_2	Thickness (m) of layer_2
...	...
THK_N-1	Thickness (m) of layer_N-1
THK_STD_1	STD on thickness of layer_1
THK_STD_2	STD on thickness of layer_2
...	...
THK_STD_N-1	STD on thickness of layer_N-1
DEP_BOT_STD_1	STD on depth bottom of layer_1
DEP_BOT_STD_2	STD on depth bottom of layer_2
...	...
DEP_BOT_STD_N-1	STD on depth bottom of layer_N-1
DOI_CONSERVATIVE	DOI Conservative for resistivity/conductivity
DOI_STANDARD	DOI Standard for resistivity/conductivity

The *_dat.xyz file use the following format:

Header section:

```
/INFO
/Aarhus SPIA export file. File created: 30-03-2023 13:00:34. Exported from SPIA64
/SPIA VERSION          3.7.0.0
/PROJECT NAME          ProjectName.gdb
/DUMMY
/9999
/DATATYPE              Type of data
/COORDINATE SYSTEM     Coordinate System: WGS 84 UTM zone 19S (epsg:32719)
/NUMBER OF LAYERS      30 Number of layers
/MODEL UNIT            Base unit used for resistivities: /Resistivity (Ohm-m) / conductivity
(mS/m)
/LENGTH UNIT          Base unit used for distances: Meter
```

Main section:

```
LINE_NO                Line number (always 0)
MODEL_NAME              Model Name
UTMX                    UTMX
UTMY                    UTMY
DATE                   Dummy value
TIME                   Dummy value
RECORD                 Record
ELEVATION              Topography
NUMDATA                Number of gates inverted
SEGMENT                Moment ID (3 or 5)
RESDATA                Data misfit (normalized with STD)
RESTOTAL               Total misfit
DATA_1                 Voltage (V/Am^4), for gate_1
DATA_2                 Voltage (V/Am^4), for gate_2
...
DATA_N                 Voltage (V/Am^4), for gate_N
DATASTD_1              STD on voltage, for gate_1
DATASTD_2              STD on voltage, for gate_2
...
DATASTD_N              STD on voltage, for gate_N
```

Appendix B: Vegetation and Wildlife Photos



Shorebirds in shallow water of basin- October 11, 2024



Vegetation growth in and around basin- October 11, 2024



Birds in flight over basin- October 18, 2024



Vegetation in and around basin- October 25, 2024



Animal tracks observed near basin- November 7, 2024